

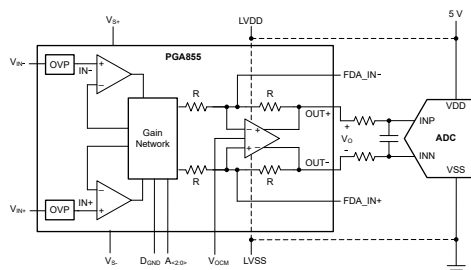
# PGA855 低ノイズ、広帯域、完全差動出力、プログラマブル・ゲイン計測アンプ

## 1 特長

- 8つのピン・プログラマブル・バイナリ・ゲイン
  - $G (V/V) = 1/8, 1/4, 1/2, 1, 2, 4, 8, \text{および } 16$
- "Low" ゲイン誤差ドリフト:  $G = 1V/V$  で  $1\text{ppm}/^\circ\text{C}$  (最大値)
- 完全差動出力
  - ADC 入力のオーバードライブ保護を可能にする独立した出力電源ピン
  - 出力同相モード制御
- 高速信号処理:
  - 広い帯域幅:  $10\text{MHz}$  (すべてのゲイン)
  - 高いスルーレート:  $35\text{V}/\mu\text{s}$
  - セトリング・タイム:
    - 誤差  $0.01\%$  まで  $500\text{ns}$ 、 $0.0015\%$  まで  $950\text{ns}$
  - 入力段ノイズ:  $G = 16\text{V/V}$  時に  $7.8\text{nV}/\sqrt{\text{Hz}}$
  - SNR を向上させるフィルタ・オプション
- 高低の電源電圧に対して  $\pm 40\text{V}$  までの入力過電圧保護機能
- 入力段電源電圧範囲:
  - 単一電源:  $8\text{V} \sim 36\text{V}$
  - デュアル電源:  $\pm 4\text{V} \sim \pm 18\text{V}$
- 出力段電源電圧範囲:
  - 単一電源:  $4.5\text{V} \sim 36\text{V}$
  - デュアル電源:  $\pm 2.25\text{V} \sim \pm 18\text{V}$
- 仕様温度範囲:  $-40^\circ\text{C} \sim +125^\circ\text{C}$
- 小型パッケージ:  $3\text{mm} \times 3\text{mm}$  VQFN

## 2 アプリケーション

- ファクトリ・オートメーションおよび制御
- アナログ入力モジュール
- データ・アキュイジション (DAQ)
- 試験および測定機器
- 半導体試験装置



PGA855 のアプリケーション概略図

## 3 概要

PGA855 は、完全差動出力を備えた高帯域のプログラマブル・ゲイン計測アンプです。PGA855 は、3本のデジタル・ゲイン選択ピンを使用して、 $0.125\text{V/V}$  の減衰ゲインから最大  $16\text{V/V}$  まで、8つのバイナリ・ゲイン設定を備えています。出力同相電圧は、VOCM ピンを使用して個別に設定できます。

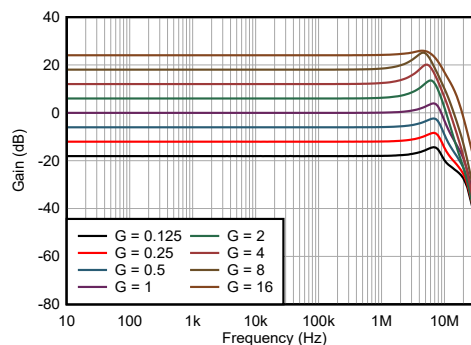
PGA855 アーキテクチャは、追加の ADC ドライバを必要とせず、最大  $1\text{MSPS}$  のサンプリング・レートで高分解能、高精度の A/D コンバータ (ADC) の入力を駆動するように最適化されています。出力段電源 (LVSS/LVDD) は入力段からデカップリングされており、ADC の電源に接続することで、オーバードライブによる損傷から ADC や下流のデバイスを保護できます。

スーパーベータ入力トランジスタが提供する入力バイアス電流は非常に低く、それにより入力電流ノイズ密度が  $0.3\text{pA}/\sqrt{\text{Hz}}$  と非常に低くなるため、PGA855 は、事実上あらゆる種類のセンサに対応する汎用性の高い選択肢になっています。低ノイズの電流フィードバック・フロントエンド・アーキテクチャにより、高周波数でも優れたゲイン平坦性を実現しているため、PGA855 は、優れた高インピーダンスのセンサ読み出しデバイスとなります。入力ピンに保護回路が内蔵されており、電源電圧を最大  $\pm 40\text{V}$  上回る過電圧に対処できます。

### パッケージ情報

部品番号	パッケージ <sup>(1)</sup>	パッケージ・サイズ <sup>(2)</sup>
PGA855	RGT (VQFN, 16)	$3\text{mm} \times 3\text{mm}$

- 利用可能なパッケージについては、パッケージ・オプションについての付録を参照してください。
- パッケージ・サイズ (長さ×幅) は公称値であり、該当する場合はピンも含まれます。



ゲインと周波数との関係

## Table of Contents

<b>1 特長</b> .....	<b>1</b>	8.4 Device Functional Modes.....	<b>24</b>
<b>2 アプリケーション</b> .....	<b>1</b>	<b>9 Application and Implementation</b> .....	<b>25</b>
<b>3 概要</b> .....	<b>1</b>	9.1 Application Information.....	<b>25</b>
<b>4 Revision History</b> .....	<b>2</b>	9.2 Typical Applications.....	<b>27</b>
<b>5 Device Comparison Table</b> .....	<b>3</b>	9.3 Power Supply Recommendations.....	<b>33</b>
<b>6 Pin Configuration and Functions</b> .....	<b>3</b>	9.4 Layout.....	<b>33</b>
<b>7 Specifications</b> .....	<b>5</b>	<b>10 Device and Documentation Support</b> .....	<b>35</b>
7.1 Absolute Maximum Ratings.....	<b>5</b>	10.1 Device Support.....	<b>35</b>
7.2 ESD Ratings.....	<b>5</b>	10.2 Documentation Support.....	<b>35</b>
7.3 Recommended Operating Conditions.....	<b>5</b>	10.3 ドキュメントの更新通知を受け取る方法.....	<b>35</b>
7.4 Thermal Information.....	<b>6</b>	10.4 サポート・リソース.....	<b>35</b>
7.5 Electrical Characteristics.....	<b>6</b>	10.5 Trademarks.....	<b>35</b>
7.6 Typical Characteristics.....	<b>9</b>	10.6 静電気放電に関する注意事項.....	<b>35</b>
<b>8 Detailed Description</b> .....	<b>21</b>	10.7 用語集.....	<b>35</b>
8.1 Overview.....	<b>21</b>	<b>11 Mechanical, Packaging, and Orderable</b>	
8.2 機能ブロック図.....	<b>21</b>	<b>Information</b> .....	<b>35</b>
8.3 Feature Description.....	<b>22</b>		

## 4 Revision History

資料番号末尾の英字は改訂を表しています。その改訂履歴は英語版に準じています。

<b>Changes from Revision A (September 2023) to Revision B (September 2023)</b>	<b>Page</b>
• 「概要」セクションで 4MSPS を 1MSPS に変更 .....	<b>1</b>
• Changed 4 MSPS to 1 MSPS in <i>Overview</i> section.....	<b>21</b>

<b>Changes from Revision * (April 2023) to Revision A (September 2023)</b>	<b>Page</b>
• PGA855 のステータスを事前情報 (プレビュー) から量産データ (アクティブ) に変更.....	<b>1</b>

## 5 Device Comparison Table

DEVICE	DESCRIPTION	GAIN EQUATION	RG PINS AT PIN
INA849	Ultra-low-noise (1-nV/ $\sqrt{\text{Hz}}$ ), high-bandwidth instrumentation amplifier	$G = 1 + 6 \text{ k}\Omega / \text{RG}$	2, 3
INA851	Low-noise (3.2 nV/ $\sqrt{\text{Hz}}$ ), high-speed (22 MHz), fully-differential instrumentation amp with overvoltage protection ( $\pm 40 \text{ V}$ )	$G = 1 + 6 \text{ k}\Omega / \text{RG}$	2, 3
PGA280	20-mV to $\pm 10\text{-V}$ programmable gain instrumentation amplifier with 3-V or 5-V differential output; analog supply up to $\pm 18 \text{ V}$	Digitally programmable with SPI	N/A
PGA281	Zero-drift, high-voltage programmable gain amplifier	Digitally pin-programmable	N/A

## 6 Pin Configuration and Functions

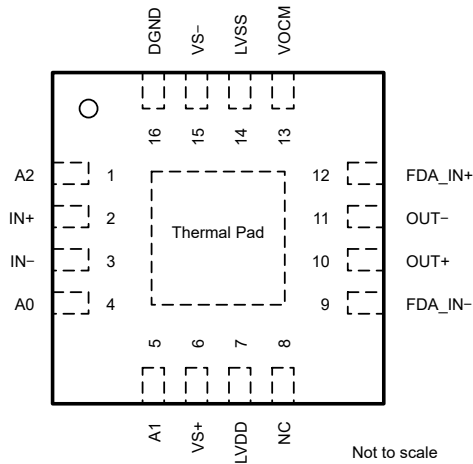


図 6-1. RGT Package, 16-Pin VQFN (Top View)

表 6-1. Pin Functions

PIN		TYPE	DESCRIPTION
NAME	NO.		
A0	4	Input	Gain option pin 0
A1	5	Input	Gain option pin 1
A2	1	Input	Gain option pin 2
DGND	16	Power	Ground reference for digital logic and gain setting pins
FDA_IN-	9	Input	Connection to output driver summing node
FDA_IN+	12	Input	Connection to output driver summing node
IN-	3	Input	Negative (inverting) input
IN+	2	Input	Positive (noninverting) input
LVDD	7	Power	Output driver positive supply. Connect this pin to the positive supply of the ADC to protect from overdriving.
LVSS	14	Power	Output driver negative supply. Connect this pin to the negative supply of the ADC to protect from overdriving.
NC	8	—	Do not connect
OUT-	11	Output	Output (inverting)
OUT+	10	Output	Output (noninverting)
VOCM	13	Input	Level set for output common mode value
VS+	6	Power	Input stage positive supply
VS-	15	Power	Input stage negative supply

表 6-1. Pin Functions (続き)

PIN		TYPE	DESCRIPTION
NAME	NO.		
Thermal Pad	Thermal pad	—	The thermal pad must be soldered to the printed-circuit board (PCB). Connect thermal pad to a plane or large copper pour that is either floating or electrically connected to VS–, even for applications that have low power dissipation.

## 7 Specifications

### 7.1 Absolute Maximum Ratings

over operating free-air temperature range (unless otherwise noted)<sup>(1)</sup>

		MIN	MAX	UNIT
V <sub>S</sub>	Supply voltage on V <sub>S+</sub> , V <sub>S-</sub> pins; V <sub>S</sub> = (V <sub>S+</sub> ) – (V <sub>S-</sub> )	0	40	V
V <sub>SOUT</sub>	Supply voltage on LVDD, LVSS pins; V <sub>SOUT</sub> = V <sub>LVDD</sub> – V <sub>LVSS</sub>	0	40	V
	Voltage on power pins LVDD, LVSS	(V <sub>S-</sub> ) – 0.5	(V <sub>S+</sub> ) + 0.5	V
V <sub>IN</sub>	Voltage on signal-input pins IN+, IN–	(V <sub>S-</sub> ) – 40	(V <sub>S+</sub> ) + 40	V
	DGND, FDA_IN+, FDA_IN– pin voltage	(V <sub>S-</sub> ) – 0.5	(V <sub>S+</sub> ) + 0.5	V
	Voltage on gain-select pins A2, A1, A0	V <sub>DGND</sub> – 0.5	(V <sub>S+</sub> ) + 0.5	V
V <sub>O</sub>	Signal output pins maximum voltage on OUT+, OUT–	V <sub>LVSS</sub> – 0.5	V <sub>LVDD</sub> + 0.5	V
V <sub>OCM</sub>	Output common-mode voltage	V <sub>LVSS</sub> – 0.5	V <sub>LVDD</sub> + 0.5	V
I <sub>O</sub>	Signal-output pins current	–100	100	mA
I <sub>SC</sub>	Output short-circuit current <sup>(2)</sup>	Continuous		
T <sub>A</sub>	Operating temperature	–50	150	°C
T <sub>J</sub>	Junction Temperature		175	°C
T <sub>stg</sub>	Storage Temperature	–65	150	°C

- (1) Operation outside the *Absolute Maximum Ratings* may cause permanent device damage. Absolute Maximum Ratings do not imply functional operation of the device at these or any other conditions beyond those listed under *Recommended Operating Conditions*. If used outside the *Recommended Operating Conditions* but within the *Absolute Maximum Ratings*, the device may not be fully functional, and this may affect device reliability, functionality, performance, and shorten the device lifetime.
- (2) Short-circuit to V<sub>SOUT</sub> / 2.

### 7.2 ESD Ratings

			VALUE	UNIT
V <sub>(ESD)</sub>	Electrostatic discharge	Human-body model (HBM), per ANSI/ESDA/JEDEC JS-001 <sup>(1)</sup>	±2000	V
		Charged-device model (CDM), per ANSI/ESDA/JEDEC JS-002 <sup>(2)</sup>	±1000	

- (1) JEDEC document JEP155 states that 500-V HBM allows safe manufacturing with a standard ESD control process.
- (2) JEDEC document JEP157 states that 250-V CDM allows safe manufacturing with a standard ESD control process.

### 7.3 Recommended Operating Conditions

over operating free-air temperature range (unless otherwise noted)

			MIN	MAX	UNIT
V <sub>S</sub>	Input stage supply voltage	Single supply	8	36	V
		Dual supply	±4	±18	
V <sub>SOUT</sub>	Output stage supply voltage	Single supply	4.5	36	V
		Dual supply	±2.25	±18	
T <sub>A</sub>	Specified temperature		–40	125	°C

## 7.4 Thermal Information

THERMAL METRIC <sup>(1)</sup>		PGA855	UNIT
		RGT (VQFN)	
		16 PINS	
R <sub>θJA</sub>	Junction-to-ambient thermal resistance	47.3	°C/W
R <sub>θJC(top)</sub>	Junction-to-case (top) thermal resistance	53.6	°C/W
R <sub>θJB</sub>	Junction-to-board thermal resistance	22.0	°C/W
ψ <sub>JT</sub>	Junction-to-top characterization parameter	1.4	°C/W
ψ <sub>JB</sub>	Junction-to-board characterization parameter	22.0	°C/W
R <sub>θJC(bot)</sub>	Junction-to-case (bottom) thermal resistance	7.8	°C/W

(1) For information about traditional and new thermal metrics, see the [Semiconductor and IC Package Thermal Metrics](#) application report.

## 7.5 Electrical Characteristics

at T<sub>A</sub> = 25 °C, V<sub>S</sub> = V<sub>SOUT</sub> = ±15 V, V<sub>ICM</sub> = V<sub>OCM</sub> is at mid-supply, R<sub>L</sub> = 10 kΩ, and G = 1 V/V (unless otherwise noted)

PARAMETER		TEST CONDITIONS		MIN	TYP	MAX	UNIT
<b>INPUT</b>							
V <sub>OS</sub>	Differential offset voltage (input referred)	G = 1 to 16			±70	±350	μV
		G < 1			±70/G	±350/G	
	Differential offset voltage drift (input referred)	G = 1 to 16, T <sub>A</sub> = -40°C to +125°C			±0.3	±1.0	μV/°C
		G < 1, T <sub>A</sub> = -40°C to +125°C			±0.3/G	±1.0/G	
PSRR	Power-supply rejection ratio	±4 V ≤ V <sub>S</sub> ≤ ±18 V, RTI	G = 0.125	102	108	dB	
			G = 0.25	108	114		
			G = 0.5	114	120		
			G = 1	120	126		
			G = 2	120	126		
			G = 4	120	132		
			G = 8	120	136		
		G = 16	120	140			
Z <sub>id</sub>	Differential impedance				100    1		GΩ    pF
Z <sub>ic</sub>	Common-mode impedance				100    7		GΩ    pF
V <sub>I</sub>	Input voltage	V <sub>S</sub> = ±4 V to ±18 V, T <sub>A</sub> = -40°C to +125°C		(V <sub>S-</sub> ) + 2.5		(V <sub>S+</sub> ) - 2.5	V
CMRR	Common-mode rejection ratio	At dc to 60 Hz, V <sub>ICM</sub> = ±10 V, T <sub>A</sub> = -40°C to +125°C, RTI	G = 0.125	64	82	dB	
			G = 0.25	70	88		
			G = 0.5	76	94		
			G = 1	82	100		
			G = 2	88	106		
			G = 4	94	112		
			G = 8	100	118		
		G = 16	106	124			
<b>BIAS CURRENT</b>							
I <sub>B</sub>	Input bias current				0.5	1.8	nA
			T <sub>A</sub> = -40°C to +125°C		1		
	Input bias current drift		T <sub>A</sub> = -40°C to +125°C			10	pA/°C
I <sub>OS</sub>	Input offset current				0.5	1	nA
			T <sub>A</sub> = -40°C to +125°C		1		
	Input offset current drift		T <sub>A</sub> = -40°C to +125°C			10	pA/°C

## 7.5 Electrical Characteristics (続き)

at  $T_A = 25^\circ\text{C}$ ,  $V_S = V_{SOUT} = \pm 15\text{ V}$ ,  $V_{ICM} = V_{OCM}$  is at mid-supply,  $R_L = 10\text{ k}\Omega$ , and  $G = 1\text{ V/V}$  (unless otherwise noted)

PARAMETER		TEST CONDITIONS		MIN	TYP	MAX	UNIT
<b>NOISE VOLTAGE</b>							
$e_{NI}$	Input-referred voltage noise density	$f = 1\text{ kHz}$	$G = 16$		7.8		nV/ $\sqrt{\text{Hz}}$
			$G = 8$		8.0		
			$G = 4$		8.6		
			$G = 2$		12.6		
			$G = 1$		21.6		
			$G = 0.5$		42		
			$G = 0.25$		84		
			$G = 0.125$		168		
$E_{NI}$	Input-referred voltage noise	$f_B = 0.1\text{ Hz to }10\text{ Hz}$	$G = 16$		0.26		$\mu\text{V}_{PP}$
			$G = 8$		0.27		
			$G = 4$		0.29		
			$G = 2$		0.44		
			$G = 1$		0.8		
			$G = 0.5$		1.6		
			$G = 0.25$		3.2		
			$G = 0.125$		6.4		
$i_N$	Input current noise density	$f = 1\text{ kHz}$			0.3		pA/ $\sqrt{\text{Hz}}$
$I_N$	Input current noise	$f_B = 0.1\text{ Hz to }10\text{ Hz}$			13		pA <sub>PP</sub>
<b>GAIN</b>							
	Differential gain range			0.125		16	V/V
$GE$	Differential gain error	$G = 0.25, 0.5, 2, 4$			$\pm 0.02$	$\pm 0.05$	%
		$G = 1$			$\pm 0.02$	$\pm 0.03$	
		$G = 0.125, 8, 16$			$\pm 0.03$	$\pm 0.07$	
	Differential gain drift	$G = 1, T_A = -40^\circ\text{C to }+125^\circ\text{C}$				$\pm 1$	ppm/ $^\circ\text{C}$
		$G = 0.125, 0.25, 0.5, 2, 4, 8, 16, T_A = -40^\circ\text{C to }+125^\circ\text{C}$					
	Differential gain nonlinearity	$G = 0.125\text{ to }16, V_{OUTDIFF} = 10\text{ V}$			2	5	ppm
		$T_A = -40^\circ\text{C to }+125^\circ\text{C}$				10	
<b>OUTPUT</b>							
$V_{OUT}$	Output voltage	No load	$V_{SOUT} = \pm 2.25\text{ V}$	$V_{LVSS} + 0.1$		$V_{LVDD} - 0.1$	V
		$R_L = 10\text{ k}\Omega$	$V_{SOUT} = \pm 2.25\text{ V}$	$V_{LVSS} + 0.2$		$V_{LVDD} - 0.2$	
			$V_{SOUT} = \pm 18\text{ V}$	$V_{LVSS} + 0.4$		$V_{LVDD} - 0.4$	
$C_L$	Load capacitance	Stable operation for differential load			50		pF
$I_{SC}$	Short-circuit current	Continuous to $V_{SOUT} / 2$			$\pm 45$		mA
			$T_A = -40^\circ\text{C to }+125^\circ\text{C}$		$\pm 20$		
<b>FREQUENCY RESPONSE</b>							
BW	Bandwidth, -3 dB	$G = 0.125\text{ to }16$			10		MHz
SR	Slew rate	$G = 0.125\text{ to }16, V_{OUTDIFF} > 5\text{ V}$			35		V/ $\mu\text{s}$
$t_S$	Settling time	$G = 0.125\text{ to }16$ $V_{INDIFF} = 10\text{-V step or}$ $V_{OUTDIFF} = 10\text{-V step}$	To 0.01%		0.7		$\mu\text{s}$
			To 0.0015%		0.95		
	Gain switching time				2		$\mu\text{s}$
THD+N	Total harmonic distortion and Noise	Differential input, $f = 10\text{ kHz}, V_O = 10\text{ V}_{PP}$			-110		dB
		Single-ended input, $f = 10\text{ kHz}, V_O = 10\text{ V}_{PP}$			-105		
HD2	Second-order harmonic distortion	Differential input, $f = 10\text{ kHz}, V_O = 10\text{ V}_{PP}$			-120		dB
		Single-ended input, $f = 10\text{ kHz}, V_O = 10\text{ V}_{PP}$			-110		
HD3	Third-order harmonic distortion	Differential input, $f = 10\text{ kHz}, V_O = 10\text{ V}_{PP}$			-120		dB
		Single-ended input, $f = 10\text{ kHz}, V_O = 10\text{ V}_{PP}$			-110		

## 7.5 Electrical Characteristics (続き)

at  $T_A = 25^\circ\text{C}$ ,  $V_S = V_{SOUT} = \pm 15\text{ V}$ ,  $V_{ICM} = V_{OCM}$  is at mid-supply,  $R_L = 10\text{ k}\Omega$ , and  $G = 1\text{ V/V}$  (unless otherwise noted)

PARAMETER		TEST CONDITIONS	MIN	TYP	MAX	UNIT
<b>OUTPUT COMMON-MODE VOLTAGE (<math>V_{OCM}</math>) CONTROL</b>						
$V_{OCM}$	Common-mode input voltage	$V_S = \pm 4\text{ V}$	$V_{LVSS} + 1.5$	$V_{LVDD} - 1.5$		V
		$V_S = \pm 18\text{ V}$	$V_{LVSS} + 2$	$V_{LVDD} - 2$		
	Small-signal bandwidth $V_{OCM}$ pin	$V_{OCM} = 100\text{ mV}_{PP}$		16		MHz
	Large-signal bandwidth $V_{OCM}$ pin	$V_{OCM} = 0.6\text{ V}_{PP}$		16		MHz
	DC output balance	$V_{OCM}$ fixed at mid-supply ( $V_O = \pm 1\text{ V}$ )		70		dB
	Input impedance $V_{OCM}$ pin			250    1		k $\Omega$    pF
	$V_{OCM}$ offset from mid-supply	$V_{OCM}$ pin floating		$\pm 1$	$\pm 3.5$	mV
	$V_{OCM}$ offset voltage	$V_{OCM} = V_{ICM}$ , $V_O = 0\text{ V}$		$\pm 1$	$\pm 3.5$	mV
	$V_{OCM}$ offset voltage drift	$V_{OCM} = V_{ICM}$ , $V_O = 0\text{ V}$ , $T_A = -40^\circ\text{C}$ to $+125^\circ\text{C}$		$\pm 20$	$\pm 40$	$\mu\text{V}/^\circ\text{C}$
<b>INPUT STAGE POWER SUPPLY</b>						
$I_{Q\_input}$	Input stage quiescent current $V_{S+}$ , $V_{S-}$	$V_{IN} = 0\text{ V}$		3	3.7	mA
		$T_A = -40^\circ\text{C}$ to $+125^\circ\text{C}$			4.5	
<b>OUTPUT STAGE POWER SUPPLY</b>						
$I_{Q\_output}$	Output stage quiescent current $V_{LVDD}$ , $V_{LVSS}$	$V_{IN} = 0\text{ V}$ , $V_{OCM}$ fixed at mid-supply		2.3	2.8	mA
		$T_A = -40^\circ\text{C}$ to $125^\circ\text{C}$			3.5	
<b>DIGITAL LOGIC</b>						
$V_{IL}$	Digital input logic low	A0, A1, A2 pins, referred to DGND	$V_{DGND}$	$V_{DGND} + 0.8$		V
$V_{IH}$	Digital input logic high	A0, A1, A2 pins, referred to DGND	$V_{DGND} + 1.8$		$V_{S+}$	V
	Digital input pin current	A0, A1, A2 pins		1.5	3	$\mu\text{A}$
$V_{DGND}$	DGND voltage		$V_{S-}$		$(V_{S+}) - 4$	V
	DGND reference current			4	10	$\mu\text{A}$



## 7.6 Typical Characteristics

at  $T_A = 25^\circ\text{C}$ ,  $V_S = V_{\text{SOUT}} = \pm 15\text{ V}$ ,  $V_{\text{ICM}} = V_{\text{OCM}} = 0\text{ V}$ ,  $R_L = 10\text{ k}\Omega$ , and  $G = 1\text{ V/V}$  (unless otherwise noted)

**表 7-1. Table of Graphs**

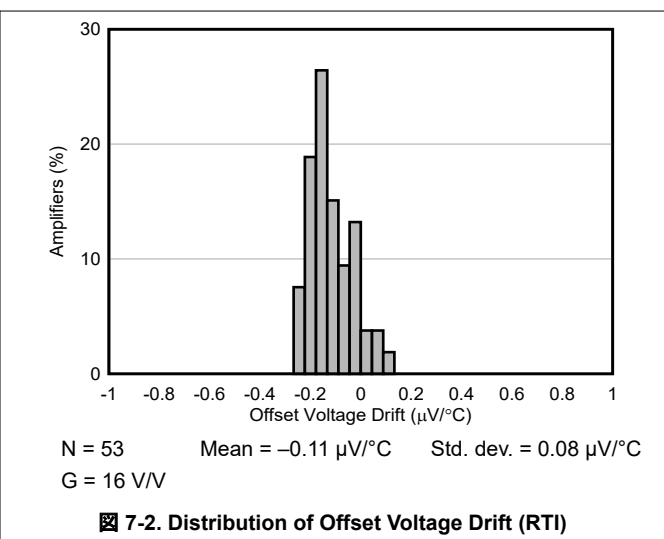
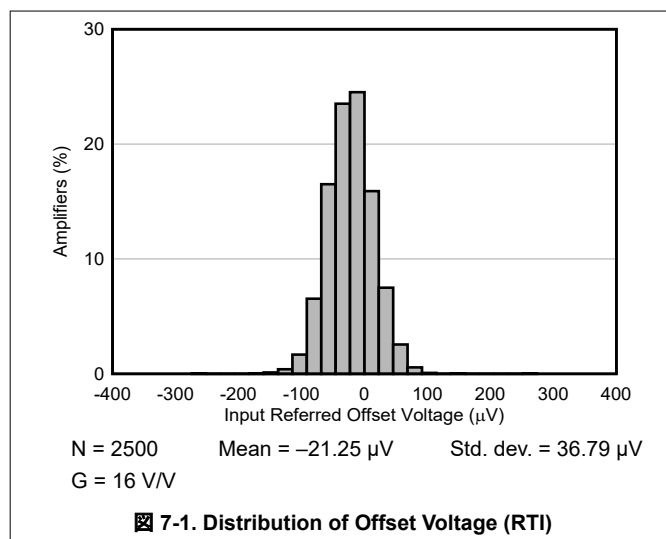
DESCRIPTION	FIGURE
Distribution of Offset Voltage (RTI), $G = 16\text{ V/V}$	<a href="#">☒ 7-1</a>
Distribution of Offset Voltage Drift (RTI), $G = 16\text{ V/V}$	<a href="#">☒ 7-2</a>
Distribution of Offset Voltage (RTI), $G = 1\text{ V/V}$	<a href="#">☒ 7-3</a>
Distribution of Offset Voltage Drift (RTI), $G = 1\text{ V/V}$	<a href="#">☒ 7-4</a>
Distribution of Offset Voltage (RTI), $G = 0.125\text{ V/V}$	<a href="#">☒ 7-5</a>
Distribution of Offset Voltage Drift (RTI), $G = 0.125\text{ V/V}$	<a href="#">☒ 7-6</a>
Distribution of Differential Gain Error, $G = 16\text{ V/V}$	<a href="#">☒ 7-7</a>
Distribution of Differential Gain Error, $G = 1\text{ V/V}$	<a href="#">☒ 7-8</a>
Gain Error vs Temperature, $G = 1\text{ V/V}$	<a href="#">☒ 7-9</a>
Distribution of Differential Gain Error, $G = 0.125\text{ V/V}$	<a href="#">☒ 7-10</a>
Distribution of Input Bias Current	<a href="#">☒ 7-11</a>
Distribution of Input Bias Current, $T_A = 85^\circ\text{C}$	<a href="#">☒ 7-12</a>
Input Bias Current vs Temperature	<a href="#">☒ 7-13</a>
Input Bias Current vs Input Common-Mode Voltage	<a href="#">☒ 7-14</a>
Distribution of Input Offset Current	<a href="#">☒ 7-15</a>
Input Offset Current vs Temperature	<a href="#">☒ 7-16</a>
Offset Voltage (RTI) vs Temperature, $G = 16\text{ V/V}$	<a href="#">☒ 7-17</a>
Offset Voltage (RTI) vs Temperature	<a href="#">☒ 7-18</a>
Offset Voltage (RTI) vs Temperature, $G = 0.125\text{ V/V}$	<a href="#">☒ 7-19</a>
Offset Voltage (RTI) vs Input Common-Mode Voltage	<a href="#">☒ 7-20</a>
CMRR Distribution, $G = 16\text{ V/V}$	<a href="#">☒ 7-21</a>
CMRR Distribution, $G = 1\text{ V/V}$	<a href="#">☒ 7-22</a>
CMRR Distribution, $G = 0.125\text{ V/V}$	<a href="#">☒ 7-23</a>
CMRR vs Frequency (RTI)	<a href="#">☒ 7-24</a>
CMRR vs Frequency (Unbalanced)	<a href="#">☒ 7-25</a>
Typical CMRR vs Temperature	<a href="#">☒ 7-26</a>
Positive PSRR vs Frequency	<a href="#">☒ 7-27</a>
Negative PSRR vs Frequency	<a href="#">☒ 7-28</a>
PSRR Distribution, $G = 16\text{ V/V}$	<a href="#">☒ 7-29</a>
PSRR Distribution, $G = 1\text{ V/V}$	<a href="#">☒ 7-30</a>
PSRR Distribution, $G = 0.125\text{ V/V}$	<a href="#">☒ 7-31</a>
Gain Nonlinearity, $G = 16\text{ V/V}$	<a href="#">☒ 7-32</a>
Gain Nonlinearity, $G = 1\text{ V/V}$	<a href="#">☒ 7-33</a>
Gain Nonlinearity, $G = 0.125\text{ V/V}$	<a href="#">☒ 7-34</a>
Voltage Noise Spectral Density (RTI) vs Frequency	<a href="#">☒ 7-35</a>
0.1-Hz to 10-Hz Voltage Noise (RTI), $G = 16\text{ V/V}$	<a href="#">☒ 7-36</a>
0.1-Hz to 10-Hz Voltage Noise (RTI), $G = 1\text{ V/V}$	<a href="#">☒ 7-37</a>
0.1-Hz to 10-Hz Voltage Noise (RTI), $G = 0.125\text{ V/V}$	<a href="#">☒ 7-38</a>
Current Noise Spectral Density vs Frequency	<a href="#">☒ 7-39</a>

## 7.6 Typical Characteristics

at  $T_A = 25^\circ\text{C}$ ,  $V_S = V_{SOUT} = \pm 15\text{ V}$ ,  $V_{ICM} = V_{OCM} = 0\text{ V}$ ,  $R_L = 10\text{ k}\Omega$ , and  $G = 1\text{ V/V}$  (unless otherwise noted)

表 7-1. Table of Graphs (続き)

DESCRIPTION	FIGURE
Gain vs Frequency	<a href="#">図 7-40</a>
Large-Signal Step Response vs Frequency	<a href="#">図 7-41</a>
Small-Signal Step Response, $G = 16\text{ V/V}$	<a href="#">図 7-42</a>
Small-Signal Step Response, $G = 1\text{ V/V}$	<a href="#">図 7-43</a>
Small-Signal Step Response, $G = 0.125\text{ V/V}$	<a href="#">図 7-44</a>
Large-Signal Step Response	<a href="#">図 7-45</a>
Gain Switching Transient Response	<a href="#">図 7-46</a>
Output Short-Circuit Current vs Temperature	<a href="#">図 7-47</a>
Positive Output Voltage Swing vs Output Current	<a href="#">図 7-48</a>
Negative Output Voltage Swing vs Output Current	<a href="#">図 7-49</a>
Overload Recovery	<a href="#">図 7-50</a>
Closed-Loop Output Impedance vs Frequency	<a href="#">図 7-51</a>
Overshoot vs Capacitive Load	<a href="#">図 7-52</a>
Quiescent Current vs Temperature	<a href="#">図 7-53</a>
THD + Noise vs Frequency (22-kHz Filter)	<a href="#">図 7-54</a>
THD + Noise vs Frequency (500-kHz Filter)	<a href="#">図 7-55</a>
2nd Harmonic Distortion vs Frequency	<a href="#">図 7-56</a>
3rd Harmonic Distortion vs Frequency	<a href="#">図 7-57</a>
Total Harmonic Distortion vs Frequency vs Output Load	<a href="#">図 7-58</a>
Ax Digital Input Pin Current vs Ax Digital Input Pin Voltage	<a href="#">図 7-59</a>
DGND Digital Input Pin Current vs A2 Digital Input Pin Voltage	<a href="#">図 7-60</a>
Digital Input Pin Current vs Temperature	<a href="#">図 7-61</a>



## 7.6 Typical Characteristics (continued)

at  $T_A = 25^\circ\text{C}$ ,  $V_S = V_{SOUT} = \pm 15\text{ V}$ ,  $V_{ICM} = V_{OCM} = 0\text{ V}$ ,  $R_L = 10\text{ k}\Omega$ , and  $G = 1\text{ V/V}$  (unless otherwise noted)

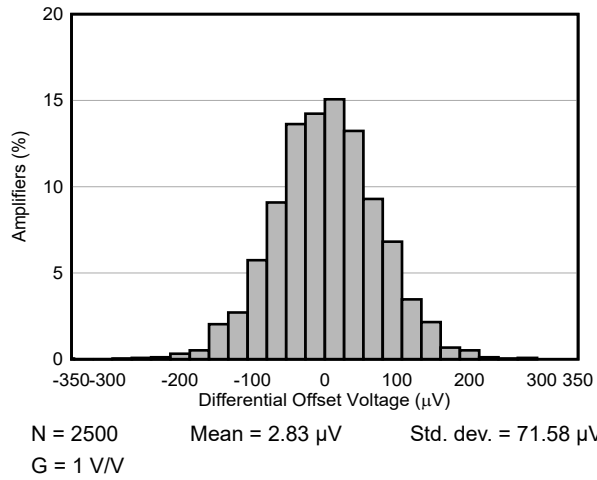


Figure 7-3. Distribution of Offset Voltage (RTI)

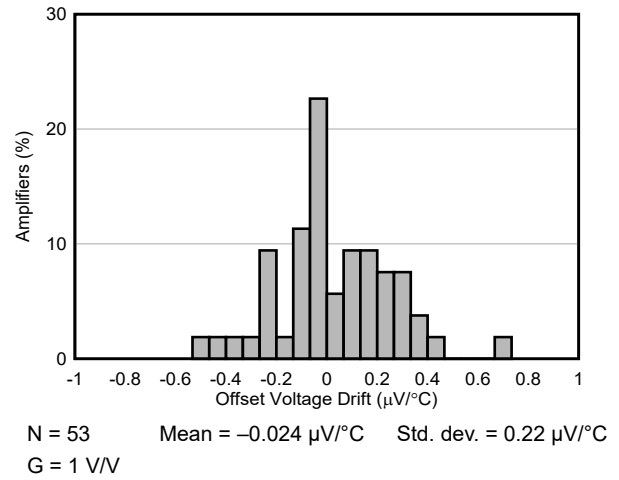


Figure 7-4. Distribution of Offset Voltage Drift (RTI)

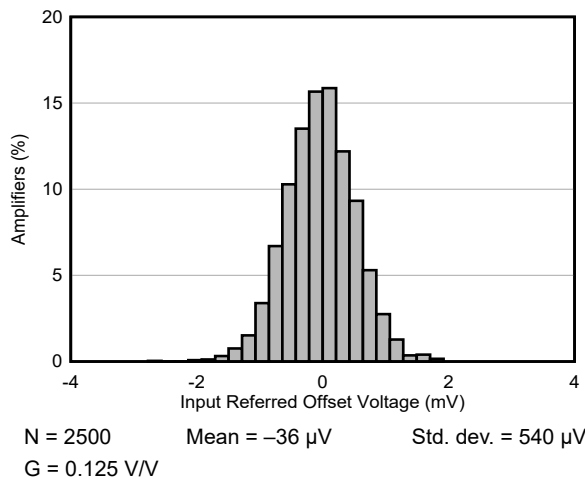


Figure 7-5. Distribution of Offset Voltage (RTI)

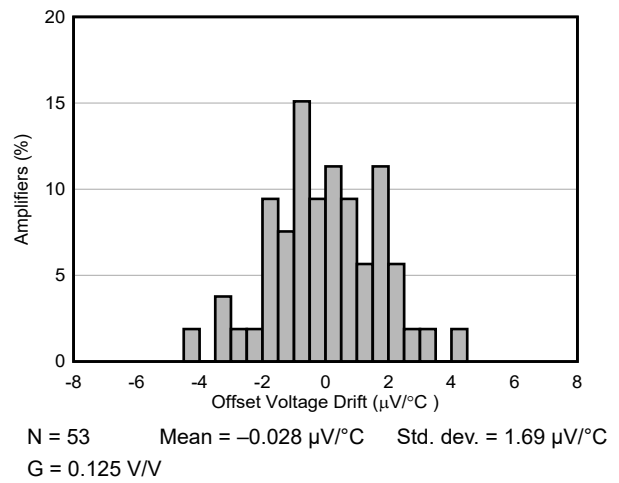


Figure 7-6. Distribution of Offset Voltage Drift (RTI)

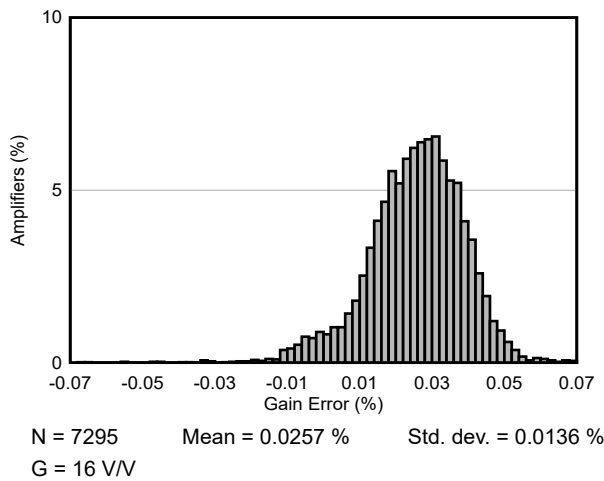


Figure 7-7. Distribution of Differential Gain Error

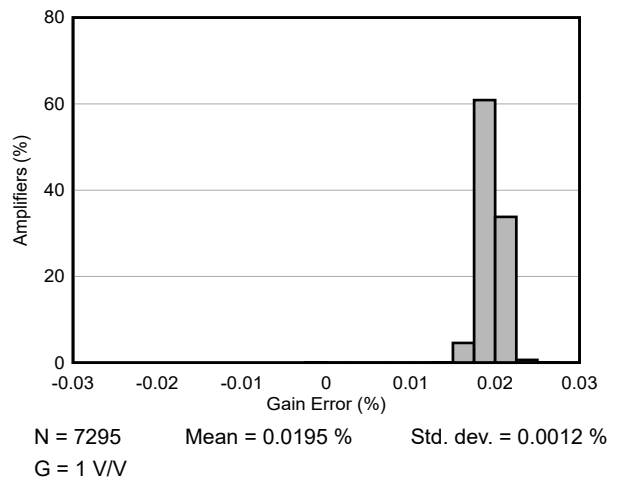


Figure 7-8. Distribution of Differential Gain Error

### 7.6 Typical Characteristics (continued)

at  $T_A = 25^\circ\text{C}$ ,  $V_S = V_{\text{SOUT}} = \pm 15\text{ V}$ ,  $V_{\text{ICM}} = V_{\text{OCM}} = 0\text{ V}$ ,  $R_L = 10\text{ k}\Omega$ , and  $G = 1\text{ V/V}$  (unless otherwise noted)

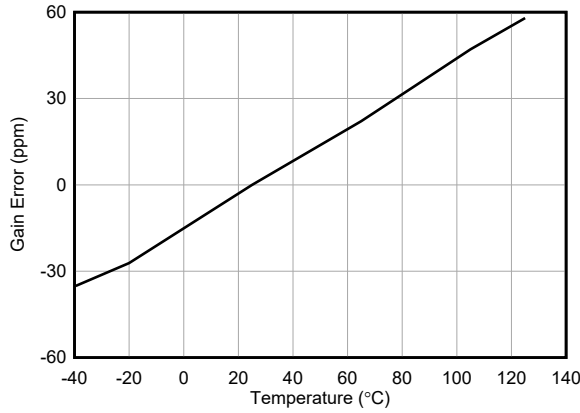


Figure 7-9. Gain Error vs Temperature

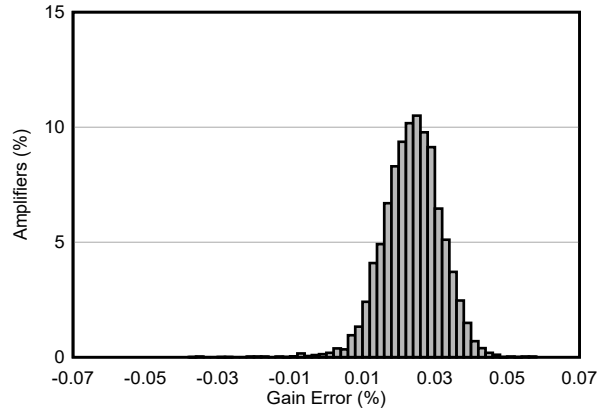


Figure 7-10. Distribution of Differential Gain Error

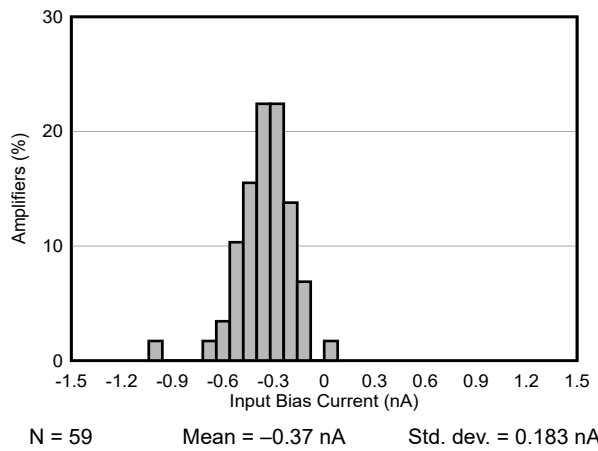


Figure 7-11. Distribution of Input Bias Current

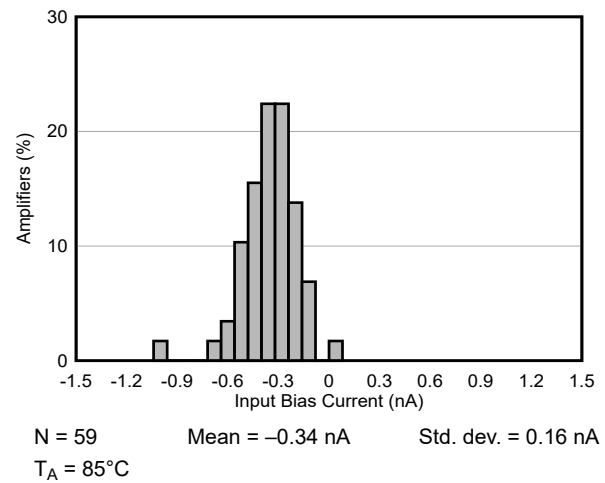


Figure 7-12. Distribution of Input Bias Current

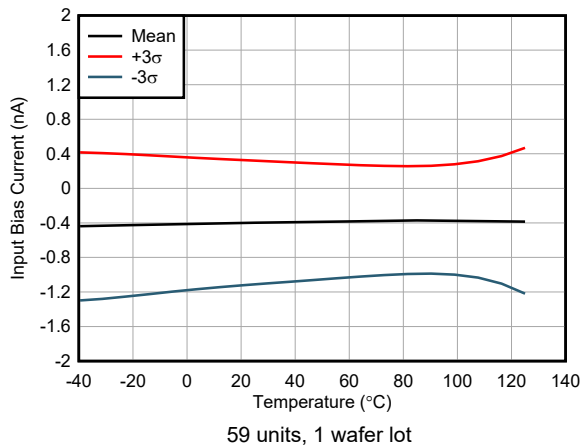


Figure 7-13. Input Bias Current vs Temperature

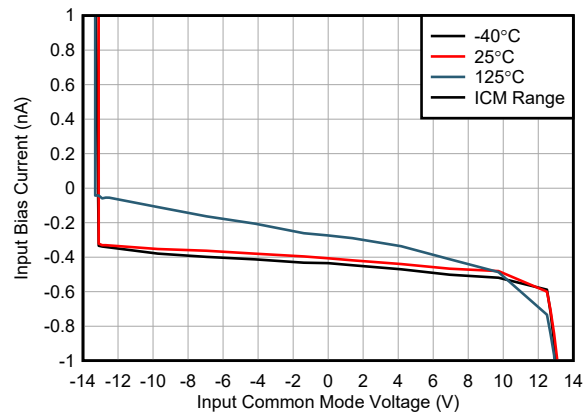
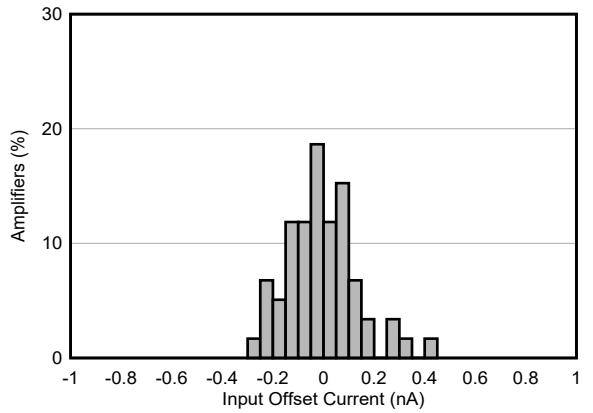


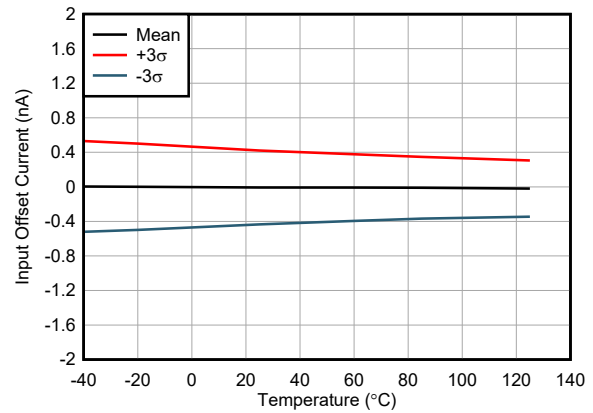
Figure 7-14. Input Bias Current vs Input Common-Mode Voltage

## 7.6 Typical Characteristics (continued)

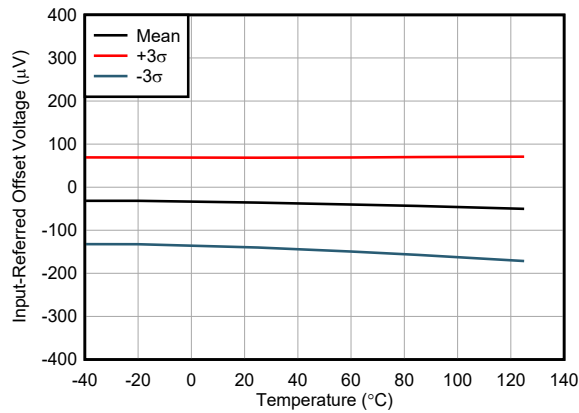
at  $T_A = 25^\circ\text{C}$ ,  $V_S = V_{SOUT} = \pm 15\text{ V}$ ,  $V_{ICM} = V_{OCM} = 0\text{ V}$ ,  $R_L = 10\text{ k}\Omega$ , and  $G = 1\text{ V/V}$  (unless otherwise noted)



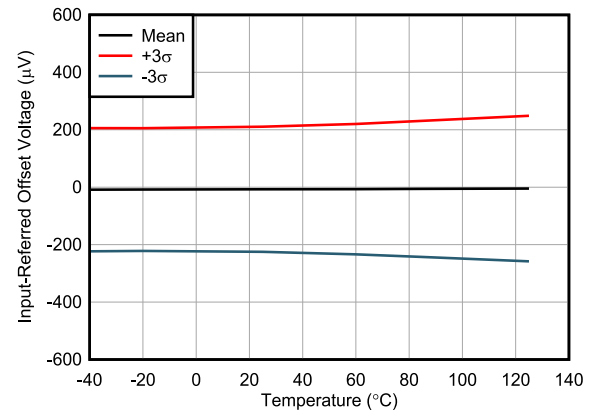
7-15. Distribution of Input Offset Current



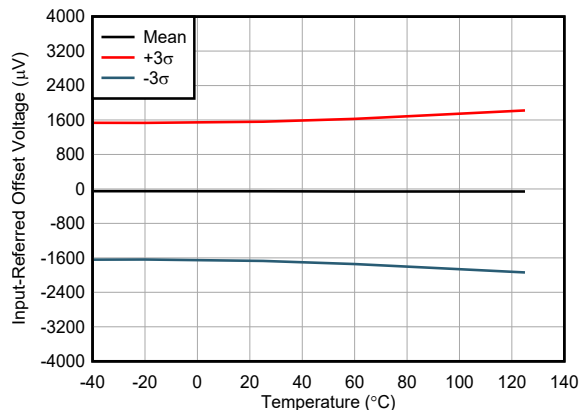
7-16. Input Offset Current vs Temperature



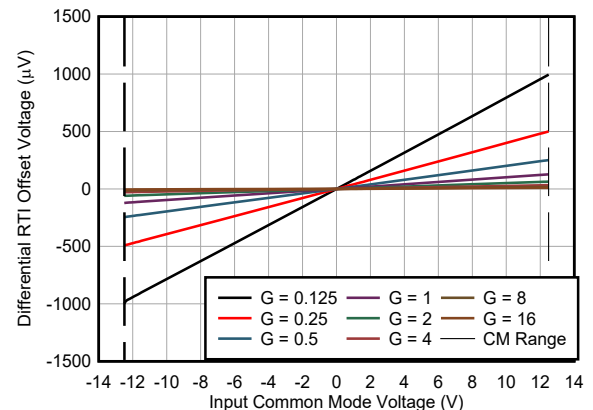
7-17. Offset Voltage (RTI) vs Temperature



7-18. Offset Voltage (RTI) vs Temperature



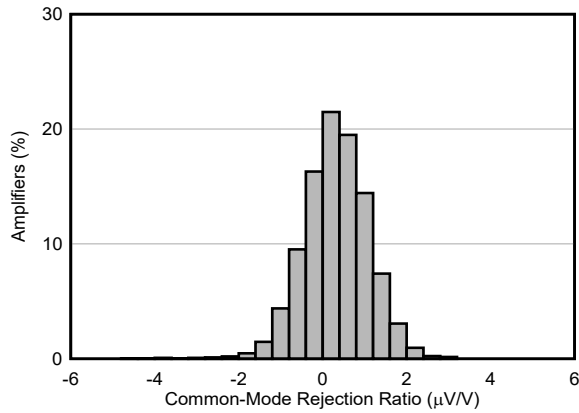
7-19. Offset Voltage (RTI) vs Temperature



7-20. Offset Voltage (RTI) vs Input Common-Mode Voltage

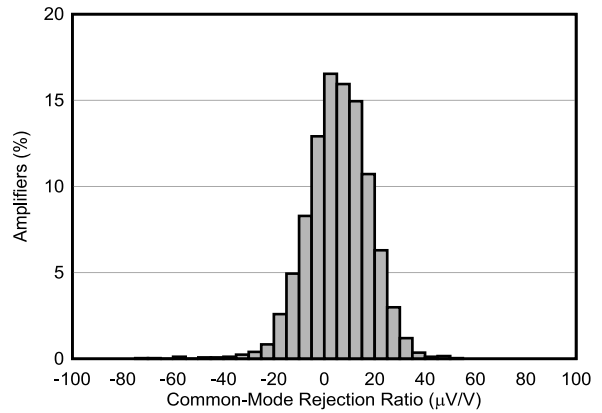
### 7.6 Typical Characteristics (continued)

at  $T_A = 25^\circ\text{C}$ ,  $V_S = V_{SOUT} = \pm 15\text{ V}$ ,  $V_{ICM} = V_{OCM} = 0\text{ V}$ ,  $R_L = 10\text{ k}\Omega$ , and  $G = 1\text{ V/V}$  (unless otherwise noted)



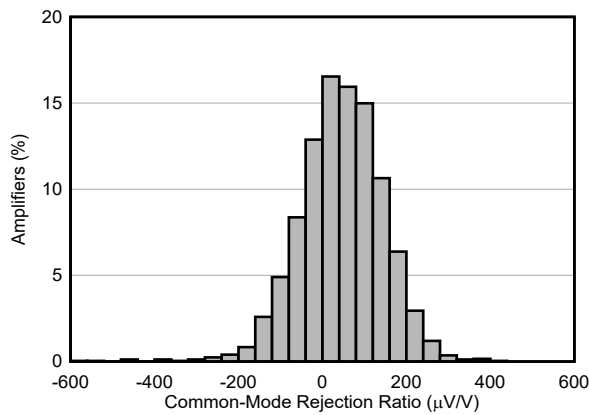
N = 2500 Mean = 0.31  $\mu\text{V/V}$  Std. dev. = 0.78  $\mu\text{V/V}$   
G = 16 V/V

7-21. CMRR Distribution



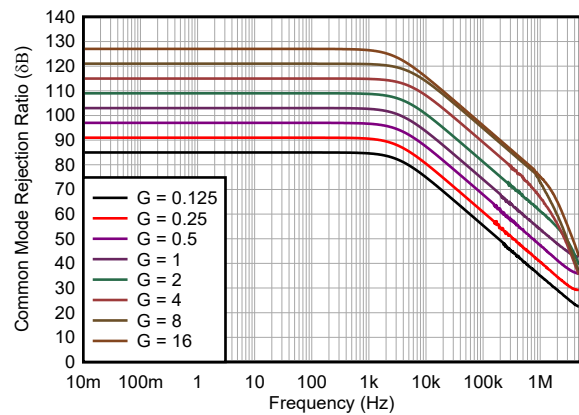
N = 2500 Mean = 5.61  $\mu\text{V/V}$  Std. dev. = 12.50  $\mu\text{V/V}$   
G = 1 V/V

7-22. CMRR Distribution

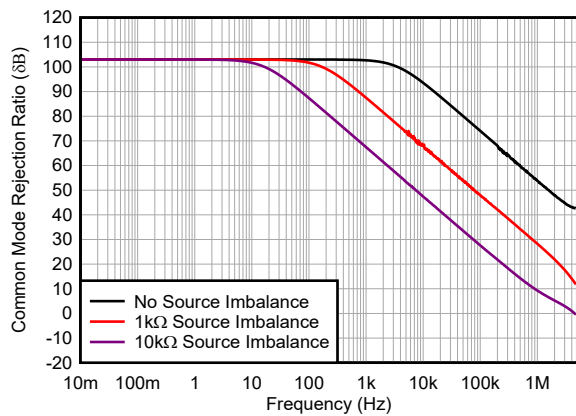


N = 2500 Mean = 44.98  $\mu\text{V/V}$  Std. dev. = 100  $\mu\text{V/V}$   
G = 0.125 V/V

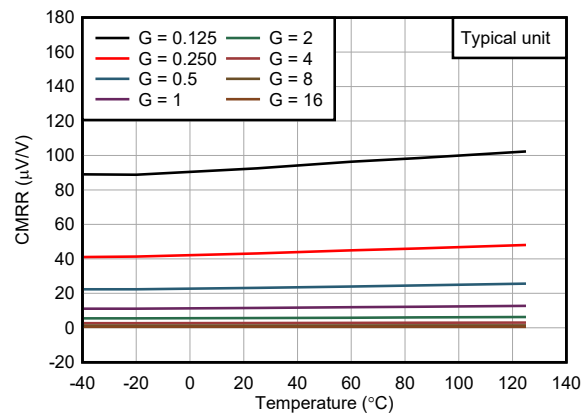
7-23. CMRR Distribution



7-24. CMRR vs Frequency (RTI)



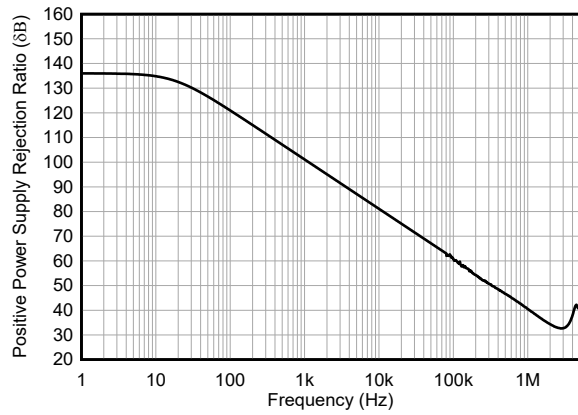
7-25. CMRR vs Frequency (Unbalanced)



7-26. Typical CMRR vs Temperature

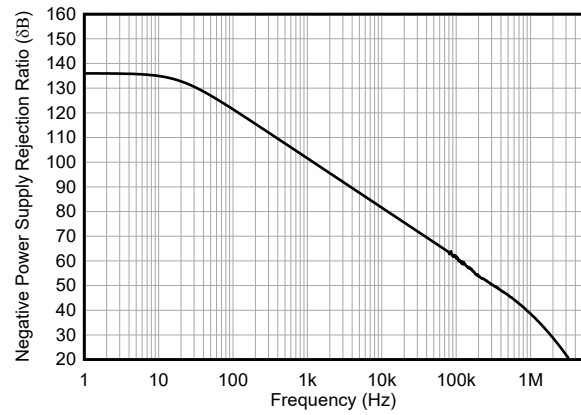
## 7.6 Typical Characteristics (continued)

at  $T_A = 25^\circ\text{C}$ ,  $V_S = V_{SOUT} = \pm 15\text{ V}$ ,  $V_{ICM} = V_{OCM} = 0\text{ V}$ ,  $R_L = 10\text{ k}\Omega$ , and  $G = 1\text{ V/V}$  (unless otherwise noted)



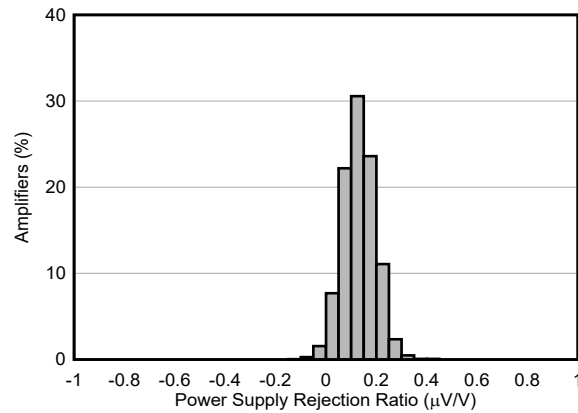
Typical unit shown

Figure 7-27. Positive PSRR vs Frequency



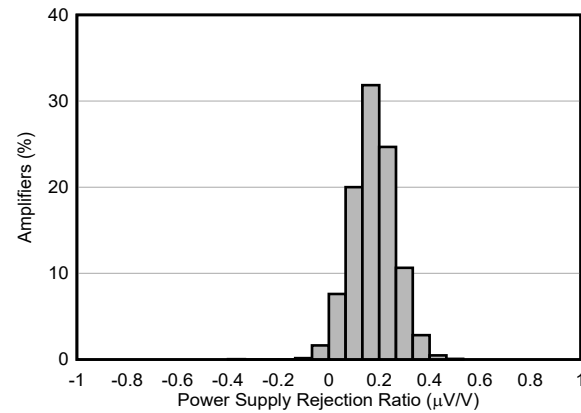
Typical unit shown

Figure 7-28. Negative PSRR vs Frequency



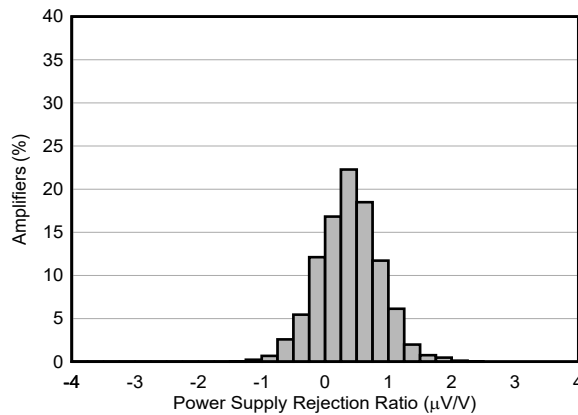
N = 2500    Mean = 0.13  $\mu\text{V/V}$     Std. dev. = 0.06  $\mu\text{V/V}$   
G = 16 V/V

Figure 7-29. PSRR Distribution



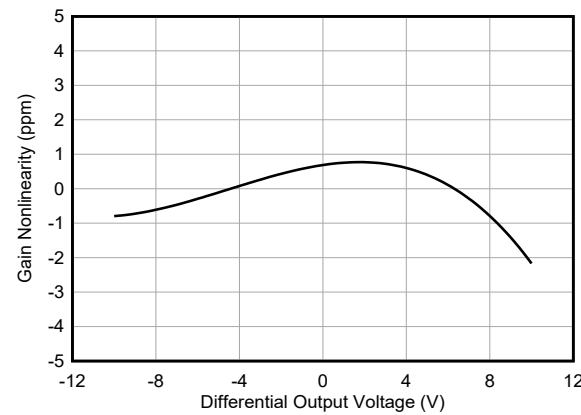
N = 2500    Mean = 0.17  $\mu\text{V/V}$     Std. dev. = 0.08  $\mu\text{V/V}$   
G = 1 V/V

Figure 7-30. PSRR Distribution



N = 2500    Mean = 0.38  $\mu\text{V/V}$     Std. dev. = 0.48  $\mu\text{V/V}$   
G = 0.125 V/V

Figure 7-31. PSRR Distribution

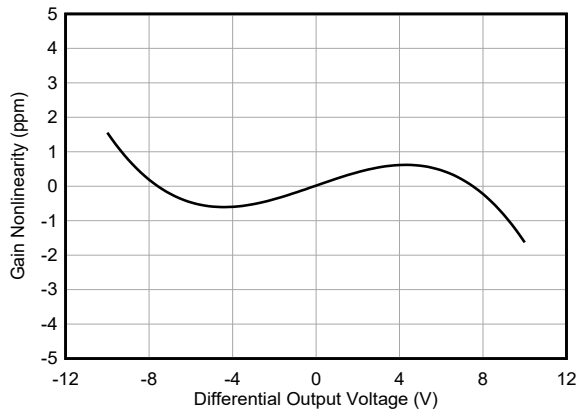


G = 16 V/V     $V_{OUTDIFF} = 10\text{ V}$

Figure 7-32. Gain Nonlinearity

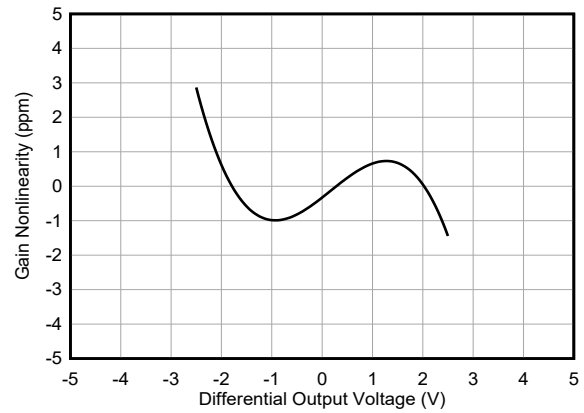
### 7.6 Typical Characteristics (continued)

at  $T_A = 25^\circ\text{C}$ ,  $V_S = V_{SOUT} = \pm 15\text{ V}$ ,  $V_{ICM} = V_{OCM} = 0\text{ V}$ ,  $R_L = 10\text{ k}\Omega$ , and  $G = 1\text{ V/V}$  (unless otherwise noted)



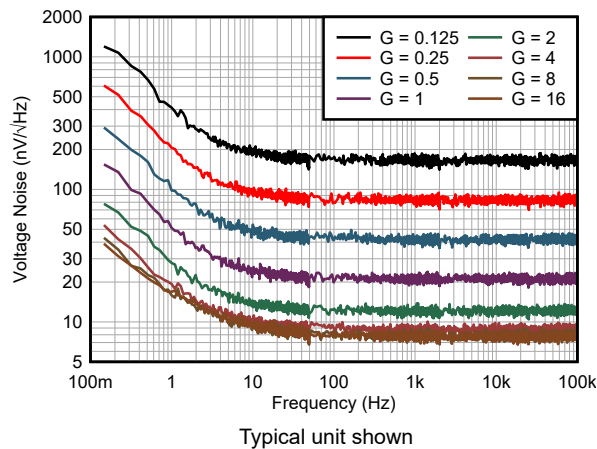
$G = 1\text{ V/V}$   $V_{OUTDIFF} = 10\text{ V}$

7-33. Gain Nonlinearity

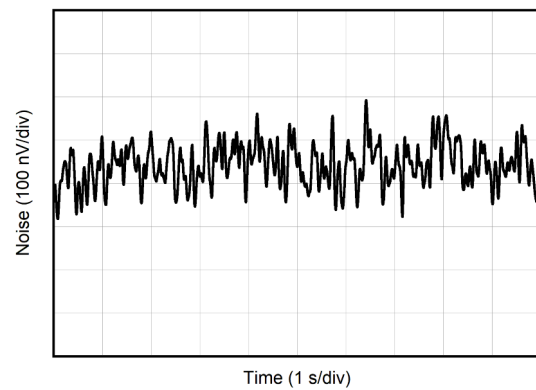


$G = 0.125\text{ V/V}$   $V_{OUTDIFF} = 2.5\text{ V}$

7-34. Gain Nonlinearity

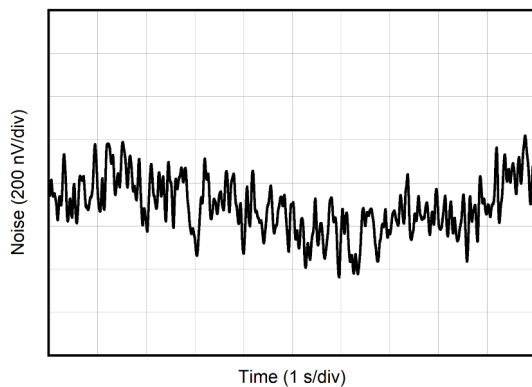


7-35. Voltage Noise Spectral Density (RTI) vs Frequency



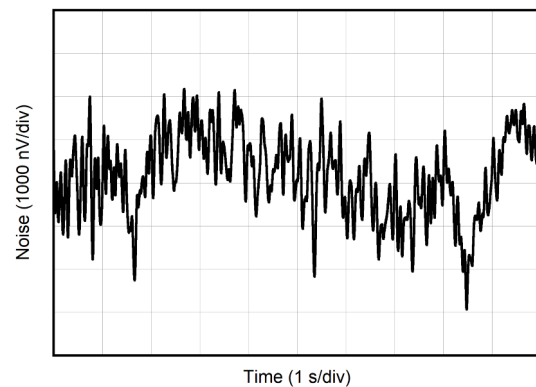
$G = 16\text{ V/V}$

7-36. 0.1-Hz to 10-Hz Voltage Noise (RTI)



$G = 1\text{ V/V}$

7-37. 0.1-Hz to 10-Hz Voltage Noise (RTI)



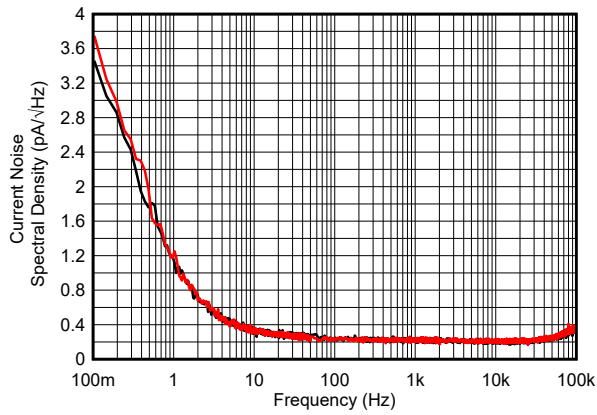
$G = 0.125\text{ V/V}$

7-38. 0.1-Hz to 10-Hz Voltage Noise (RTI)



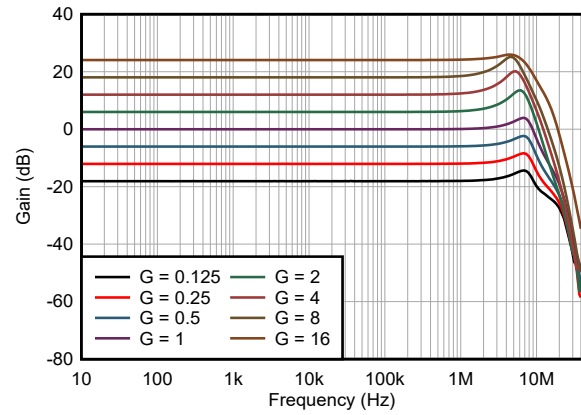
## 7.6 Typical Characteristics (continued)

at  $T_A = 25^\circ\text{C}$ ,  $V_S = V_{SOUT} = \pm 15\text{ V}$ ,  $V_{ICM} = V_{OCM} = 0\text{ V}$ ,  $R_L = 10\text{ k}\Omega$ , and  $G = 1\text{ V/V}$  (unless otherwise noted)



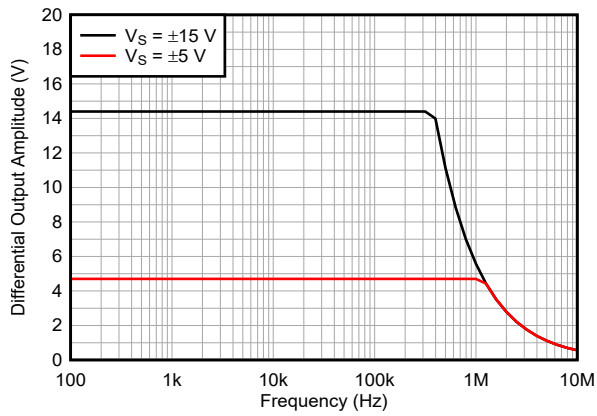
$G = 16\text{ V/V}$

Figure 7-39. Current Noise Spectral Density vs Frequency



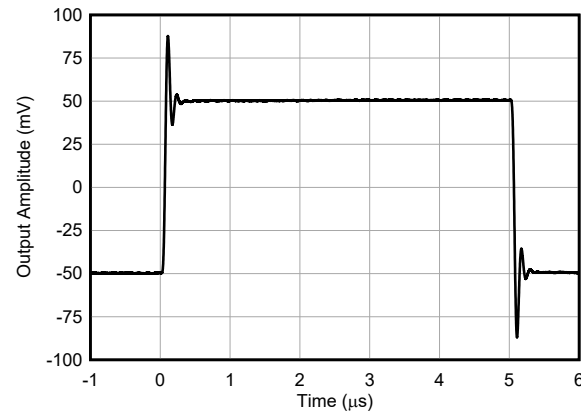
Differential load capacitance = 50 pF

Figure 7-40. Gain vs Frequency



Differential load capacitance = 50 pF

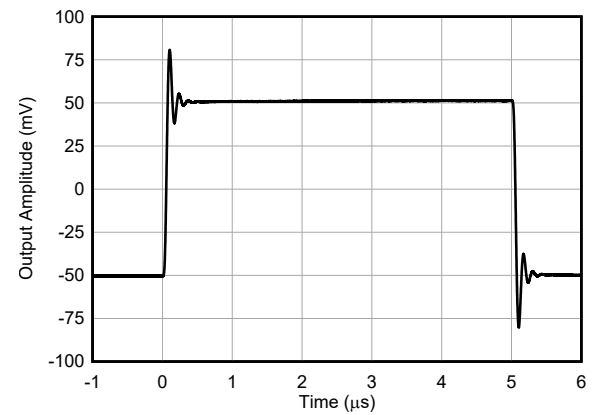
Figure 7-41. Large-Signal Step Response vs Frequency



$G = 16\text{ V/V}$

Differential load capacitance = 50 pF

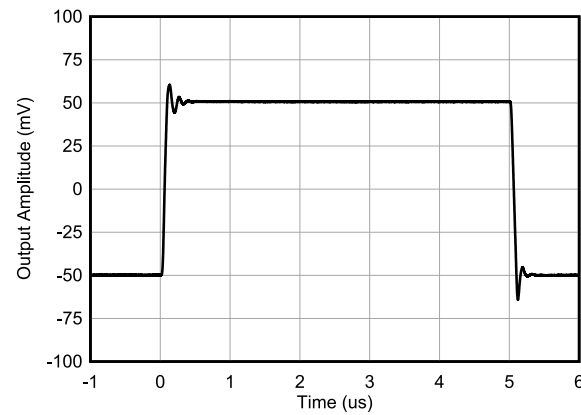
Figure 7-42. Small-Signal Step Response



$G = 1\text{ V/V}$

Differential load capacitance = 50 pF

Figure 7-43. Small-Signal Step Response



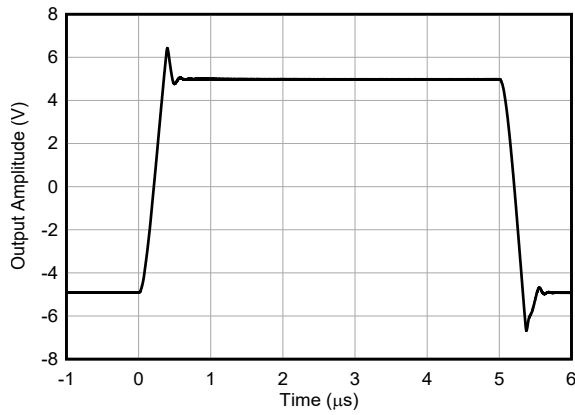
$G = 0.125\text{ V/V}$

Differential load capacitance = 50 pF

Figure 7-44. Small-Signal Step Response

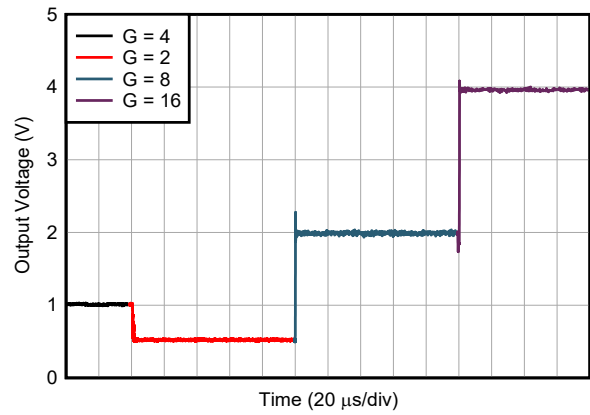
## 7.6 Typical Characteristics (continued)

at  $T_A = 25^\circ\text{C}$ ,  $V_S = V_{SOUT} = \pm 15\text{ V}$ ,  $V_{ICM} = V_{OCM} = 0\text{ V}$ ,  $R_L = 10\text{ k}\Omega$ , and  $G = 1\text{ V/V}$  (unless otherwise noted)



$G = 1\text{ V/V}$

Figure 7-45. Large-Signal Step Response



Input voltage = 250 mV<sub>pp</sub>

Figure 7-46. Gain Switching Transient Response

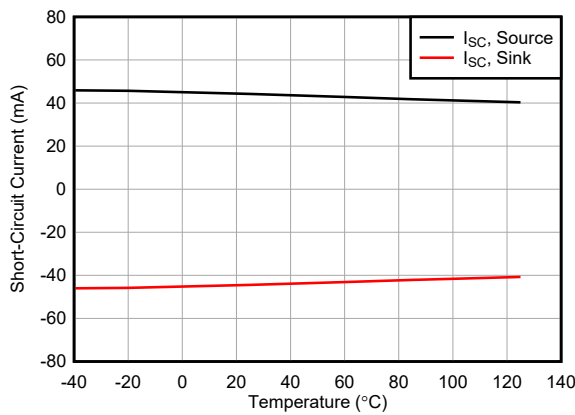
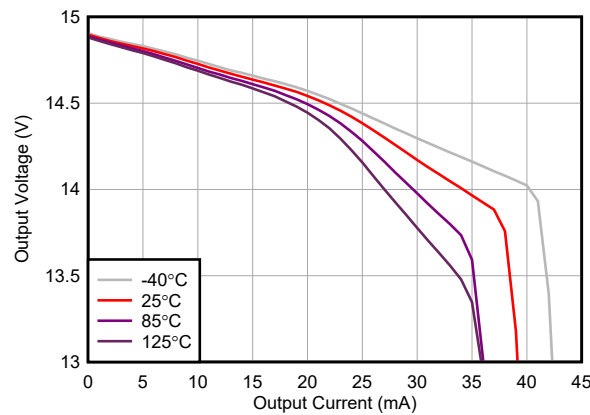


Figure 7-47. Output Short-Circuit Current vs Temperature

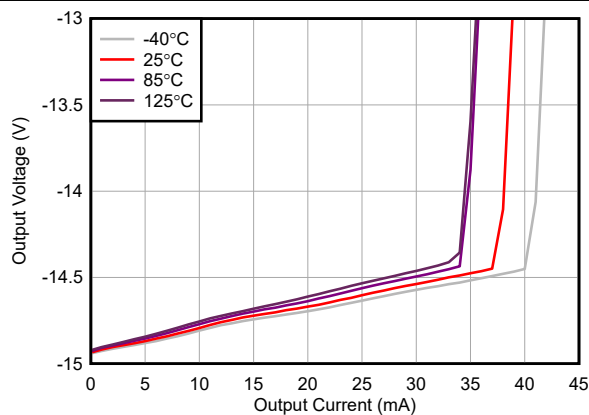


$V_S = \pm 18\text{ V}$

$V_{SOUT} = \pm 15\text{ V}$

$G = 16\text{ V/V}$

Figure 7-48. Positive Output Voltage vs Output Current



$V_S = \pm 18\text{ V}$

$V_{SOUT} = \pm 15\text{ V}$

$G = 16\text{ V/V}$

Figure 7-49. Negative Output Voltage vs Output Current

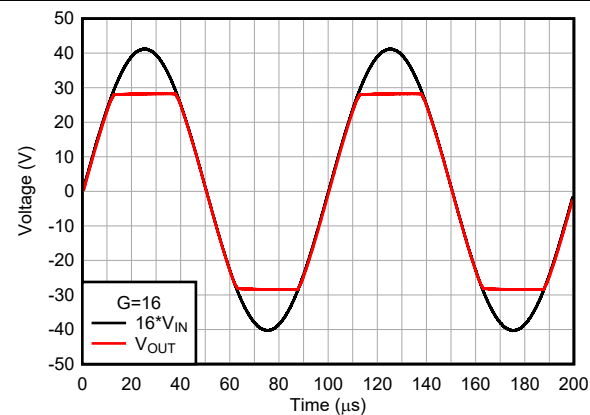
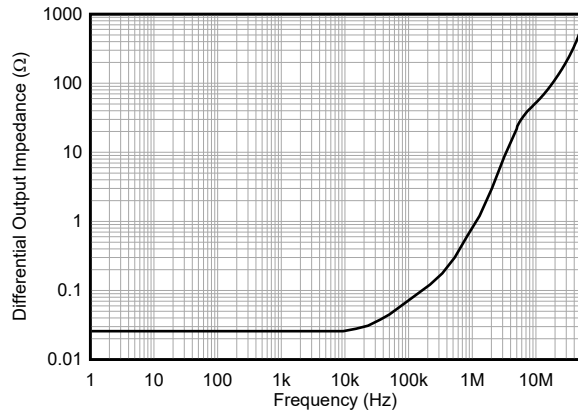


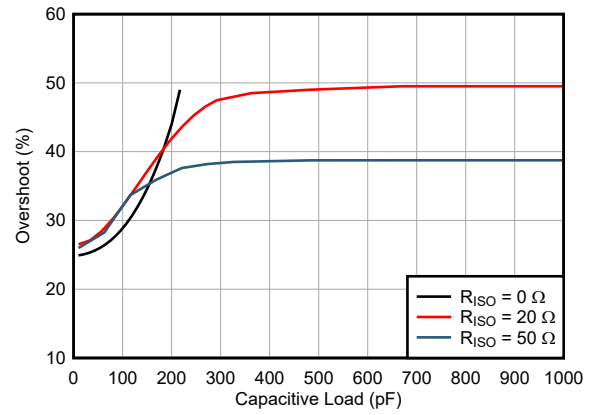
Figure 7-50. Overload Recovery

## 7.6 Typical Characteristics (continued)

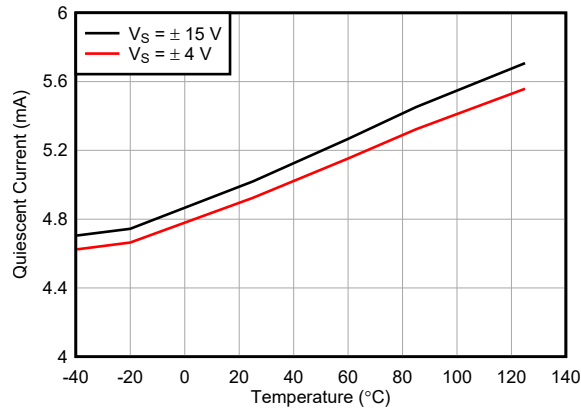
at  $T_A = 25^\circ\text{C}$ ,  $V_S = V_{SOUT} = \pm 15\text{ V}$ ,  $V_{ICM} = V_{OCM} = 0\text{ V}$ ,  $R_L = 10\text{ k}\Omega$ , and  $G = 1\text{ V/V}$  (unless otherwise noted)



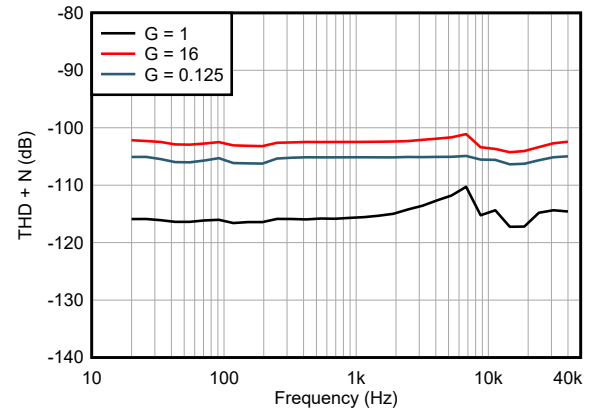
7-51. Closed Loop Output Impedance vs Frequency



7-52. Overshoot vs Capacitive Load

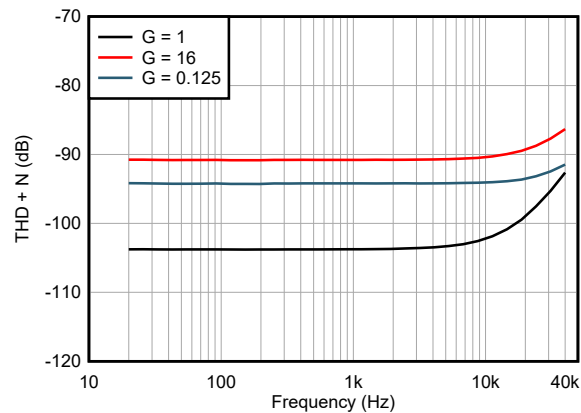


7-53. Quiescent Current vs Temperature



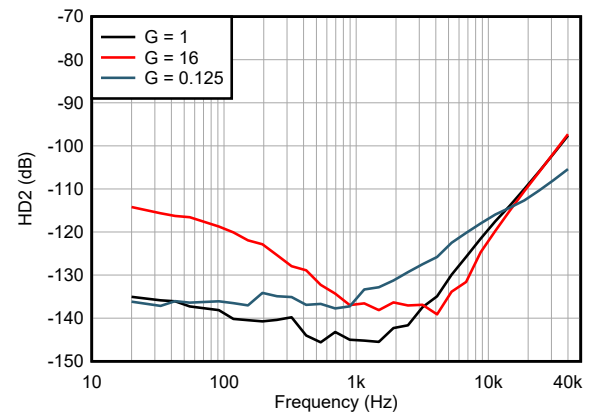
10-Hz to 22-kHz band-pass filter  $V_{OUTDIFF} > 2.5\text{ V}_{PP}$

7-54. Total Harmonic Distortion + Noise vs Frequency



10-Hz to 500-kHz band-pass filter  $V_{OUTDIFF} > 2.5\text{ V}_{PP}$

7-55. Total Harmonic Distortion + Noise vs Frequency

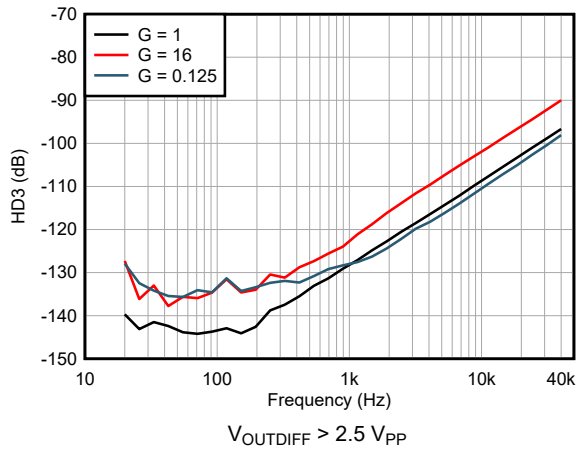


$V_{OUTDIFF} > 2.5\text{ V}_{PP}$

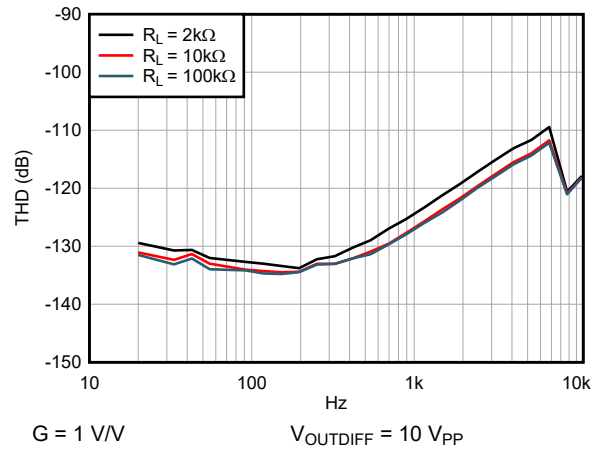
7-56. 2nd Harmonic Distortion vs Frequency

### 7.6 Typical Characteristics (continued)

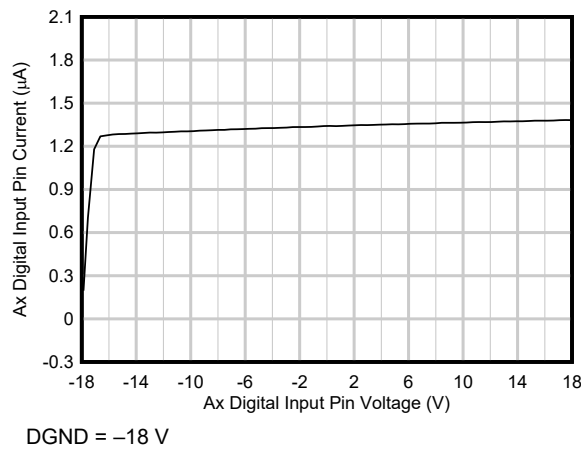
at  $T_A = 25^\circ\text{C}$ ,  $V_S = V_{\text{SOUT}} = \pm 15\text{ V}$ ,  $V_{\text{ICM}} = V_{\text{OCM}} = 0\text{ V}$ ,  $R_L = 10\text{ k}\Omega$ , and  $G = 1\text{ V/V}$  (unless otherwise noted)



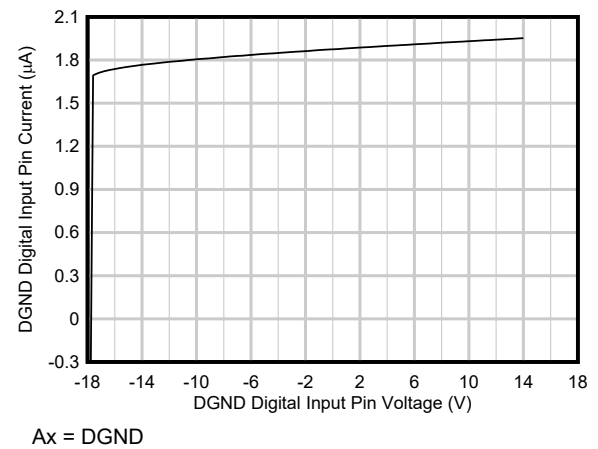
7-57. 3rd Harmonic Distortion vs Frequency



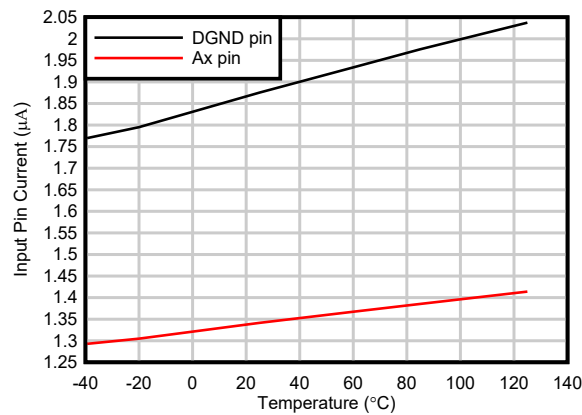
7-58. Total Harmonic Distortion vs Frequency



7-59. Ax Digital Input Pin Current vs Ax Digital Input Pin Voltage



7-60. DGND Digital Input Pin Current vs DGND Digital Input Pin Voltage



7-61. Digital Input Pin Current vs Temperature

## 8 Detailed Description

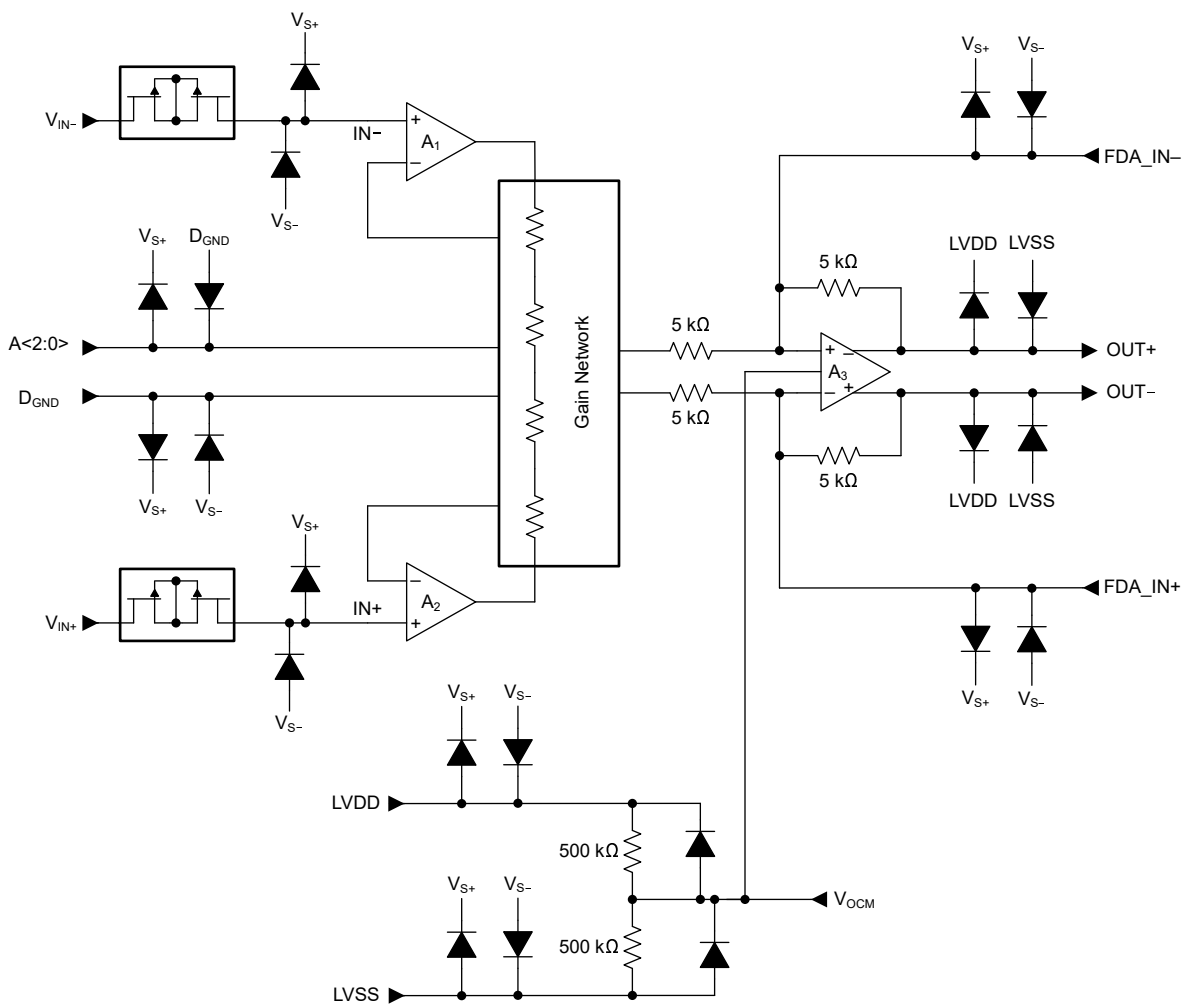
### 8.1 Overview

The PGA855 is a monolithic, high-voltage, precision programmable-gain instrumentation amplifier. The PGA855 combines a high-speed current-feedback input stage with an internally matched gain resistor network, followed by a four-resistor, fully differential amplifier output stage. Eight preprogrammed binary gains, ranging from 0.125 V/V to 16 V/V are selectable using gain-select pins A0, A1, and A2.

A functional block diagram for PGA855 is shown in the next section. The differential input voltage is fed into a pair of matched, high-impedance input-current-feedback amplifiers. An integrated precision-matched gain resistor network is used to amplify the differential input voltage. A fully differential output difference amplifier, A<sub>3</sub>, rejects the input common-mode component and refers the output signal to the voltage level set by the VO<sub>CM</sub> pin.

The PGA855 output amplifier bandwidth is optimized to drive high-performance analog-to-digital converters (ADCs) with sampling rates up to 1 MSPS without the need for an additional ADC driver. The output amplifier uses a separate power supply that is independent of the input-stage power supply. When driving an ADC, use a low-impedance connection from LVDD and LVSS to the ADC power supplies. This configuration protects the ADC inputs from damage due to inadvertent overvoltage conditions.

### 8.2 機能ブロック図



## 8.3 Feature Description

### 8.3.1 Gain Control

The PGA855 uses three pins to set the amplifier gain. These gain select pins are set with respect to DGND. This configuration simplifies design when compared to programmable-gain amplifiers requiring an SPI or other digital interface options for gain changes. [図 8-1](#) shows the gain-setting block diagram. [表 8-1](#) lists the gain options. Any gain select pin that is not driven by an external source is automatically biased at DGND using internal pulldown options.

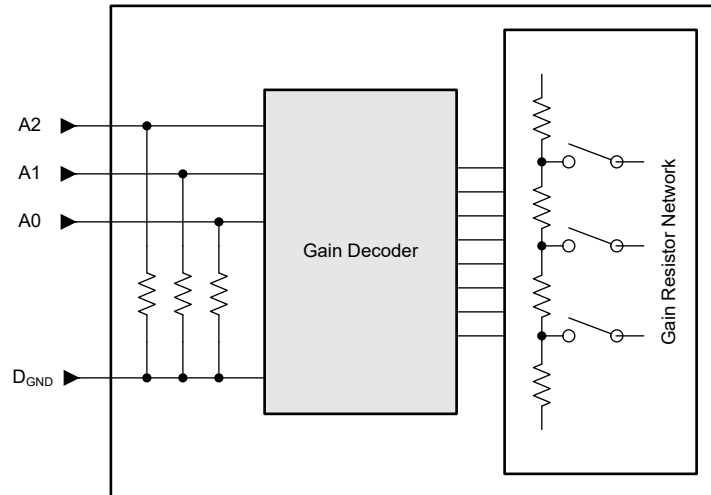


**図 8-1. PGA855 Gain Setting Block Diagram**

**表 8-1. Gain Options**

A2:A0	GAIN
000	0.125
001	0.25
010	0.5
011	1
100	2
101	4
110	8
111	16

### 8.3.2 Input Protection

The inputs of PGA855 are individually protected for voltages up to  $\pm 40$  V beyond either supply. For example, an input common-mode voltage anywhere between  $-55$  V and  $+55$  V does not cause damage when powered from  $\pm 15$ -V supplies. Internal circuitry on each input provides low series impedance under normal signal conditions, thus maintaining high performance under normal operating conditions. If the input is overloaded, the protection circuitry limits the input current to a value of approximately 4.8 mA. Figure 8-2 shows the input protection functionality during an overvoltage condition.

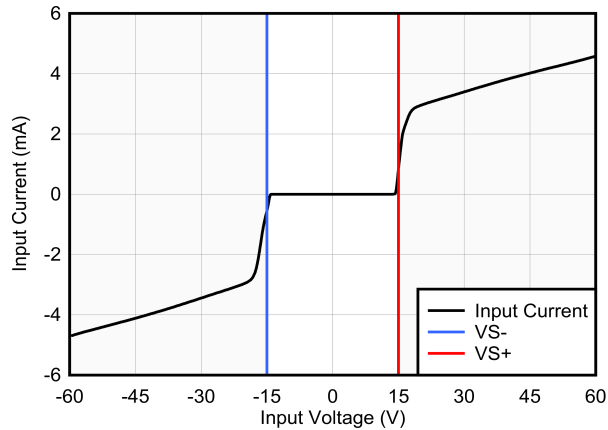


Figure 8-2. Input Current vs Input Overvoltage

Figure 8-3 shows that during an input overvoltage condition, current flows through the input protection diodes into the power supplies. In applications where the power supplies are unable to sink current, place Zener diode clamps (ZD1 and ZD2) on the power supplies to provide a current pathway to ground.

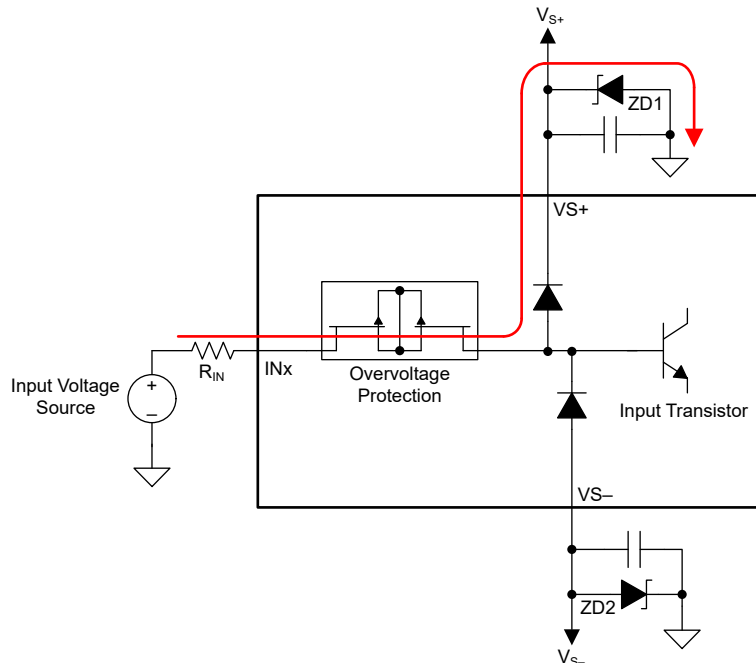


Figure 8-3. Input Current Path During an Overvoltage Condition

### 8.3.3 Output Common-Mode Pin

The output voltages of the PGA855 are balanced with respect to the voltage on the output common-mode pin, VO<sub>CM</sub>. The starting point for most designs is to assign an output common-mode voltage for the PGA855. For ac-coupled signal paths, this voltage is often the default mid-supply voltage, so as to retain the most available output swing around the voltage centered at VO<sub>CM</sub>. For dc-coupled signal paths, set this voltage between a maximum of  $V_{LVDD} - 1.5\text{ V}$  and minimum of  $V_{LVSS} + 1.5\text{ V}$ . For precision ADC applications, this voltage is typically the input common-mode voltage of the ADC.

The voltage at the VO<sub>CM</sub> pin is internally buffered to bias the fully differential output amplifier, eliminating the need for an external VO<sub>CM</sub> buffer. In the event that the VO<sub>CM</sub> pin is left floating, the output common-mode voltage is biased at output mid-supply using an internal 500-k $\Omega$  / 500-k $\Omega$  resistor divider network connected between the output-stage power-supply pins.

### 8.3.4 Using the Fully Differential Output Amplifier to Shape Noise

セクション 8.2 shows that the PGA855 output-stage fully-differential amplifier uses 5-k $\Omega$  feedback resistors between the OUT+ and OUT– outputs and the inverting and noninverting inputs, respectively. External direct access to the inverting and noninverting inputs of the fully differential amplifier is provided through the FDA\_IN– and FDA\_IN+ pins, respectively. This option allows circuit designers to add external feedback capacitors in parallel with the internal feedback resistors to implement noise-filtering or noise-shaping techniques. These pins can also be used to implement customized attenuating gains for the output stage. Consider the following important factors when designing parallel circuits with the internal feedback resistors:

- The accuracy of the internal resistor network is 0.01 % or better. This accuracy results in a common-mode rejection (CMRR) of 80 dB or better. Mismatched leakage currents on these pins can cause CMRR degradation.
- The internal resistors have  $\pm 15\%$  absolute resistance variation and must be considered when implementing custom attenuating gains or noise filters.

#### 注意

Do not treat these pins as outputs, nor use the pins to source or sink current. Excessive currents through the feedback resistors can cause permanent damage to internal circuitry.

## 8.4 Device Functional Modes

The PGA855 has a single functional mode and operates when the input-stage power supply is greater than  $\pm 4\text{ V}$  (8 V) and the output-stage power supply is greater than  $\pm 2.25\text{ V}$  (4.5 V); see also セクション 7.3.



## 9 Application and Implementation

### 注

Information in the following applications sections is not part of the TI component specification, and TI does not warrant its accuracy or completeness. TI's customers are responsible for determining suitability of components for their purposes, as well as validating and testing their design implementation to confirm system functionality.

### 9.1 Application Information

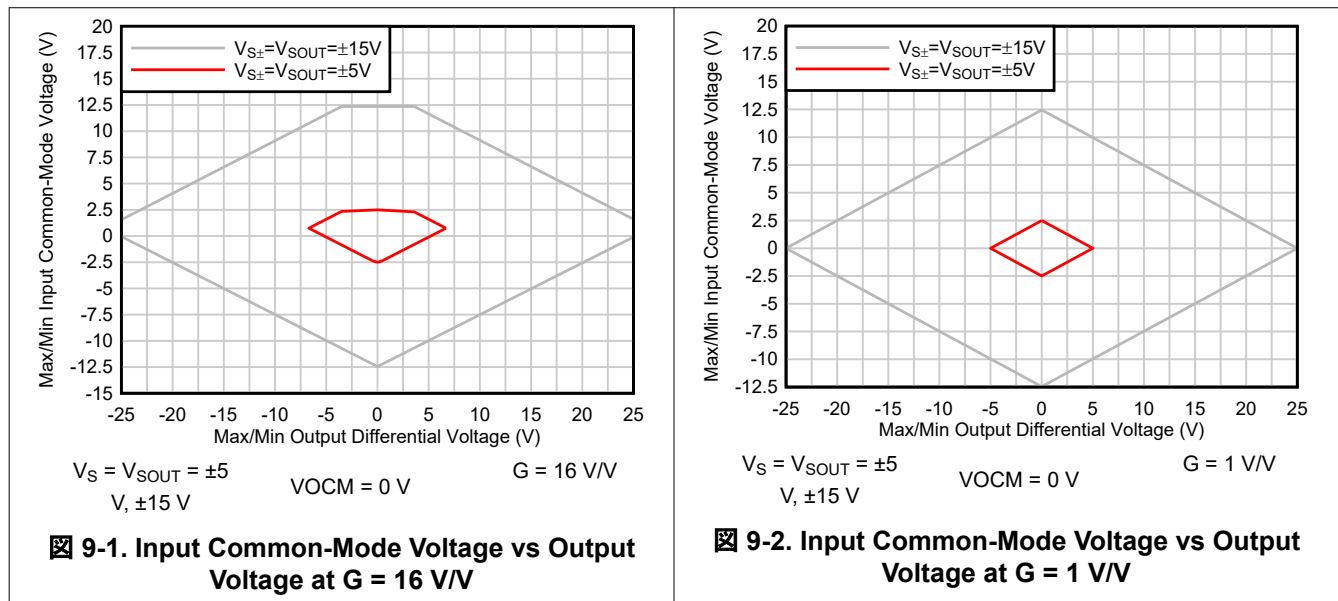
The PGA855 is a monolithic, high-voltage, high bandwidth, precision programmable gain instrumentation amplifier with fully differential outputs. The PGA855 combines a high-speed current-feedback input stage with an internally matched gain resistor network, followed by a four-resistor, fully differential amplifier output stage. The PGA855 is equipped with 8 binary-gain settings, from 0.125 V/V to 16 V/V, using three digital gain-selection pins: A0, A1, and A2.

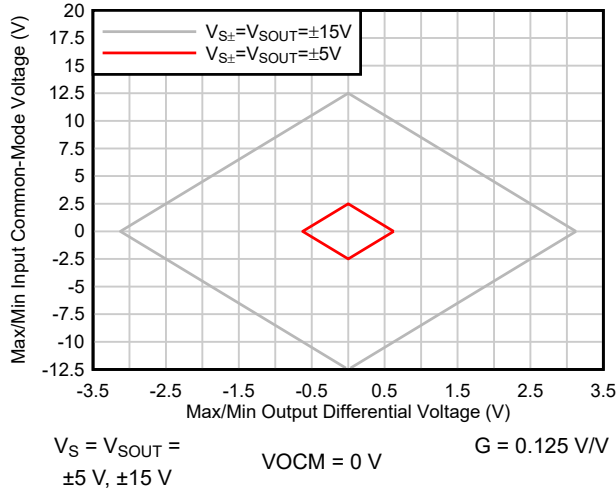
The PGA855 is designed to work with applications such as factory automation and control, analog input modules, data acquisition, test and measurement, and semiconductor test.

#### 9.1.1 Linear Operating Input Range

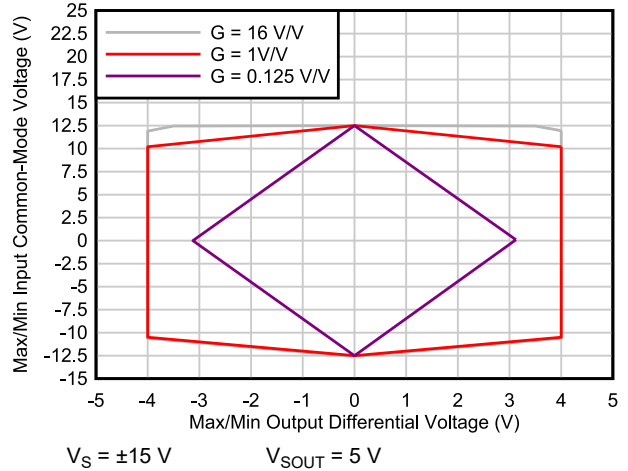
The linear operating input voltage range of the PGA855 input circuitry extends within 2.5 V (maximum) of both power supplies, and maintains excellent common-mode rejection throughout this range. The linear operating input common-mode range is a function of the input common-mode voltage, input differential voltage, gain, and output common-mode voltage.

The valid common-mode range to enable valid output voltage at no load condition are shown in [Figure 9-1](#) to [Figure 9-3](#).

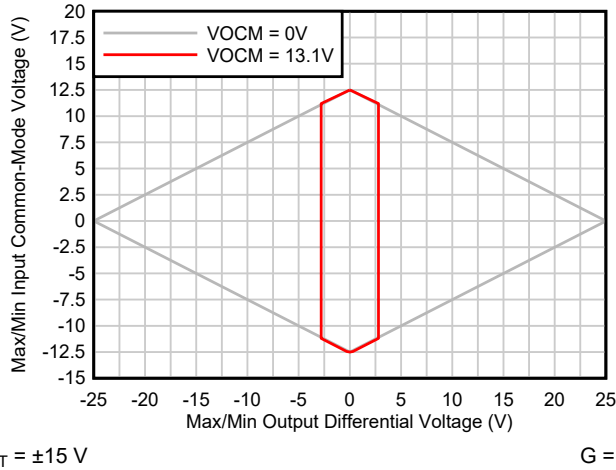




9-3. Input Common-Mode Voltage vs Output Voltage at  $G = 0.125 V/V$



9-4. Input Common-Mode Voltage vs Output Voltage at  $VOCM = 2.5V$



9-5. Input Common-Mode Voltage vs Output Voltage at  $VOCM$  max

## 9.2 Typical Applications

### 9.2.1 ADS127L11 and ADS127L21, 24-Bit, Delta-Sigma ADC Driver Circuit

The application circuit in [Figure 9-6](#) shows a schematic for a 24-bit wide-bandwidth, delta-sigma ADC. The [ADS127Lx1](#) ADC offers two digital filters to optimize ac applications (wideband filter) or dc applications (sinc4 filter). [Table 9-2](#) and [Table 9-3](#) show measurement results in both filter settings. For a detailed design procedure to operate the [ADS127Lx1](#) ADC, see the [ADS127Lx1EVM-PDK evaluation module user's guide](#).

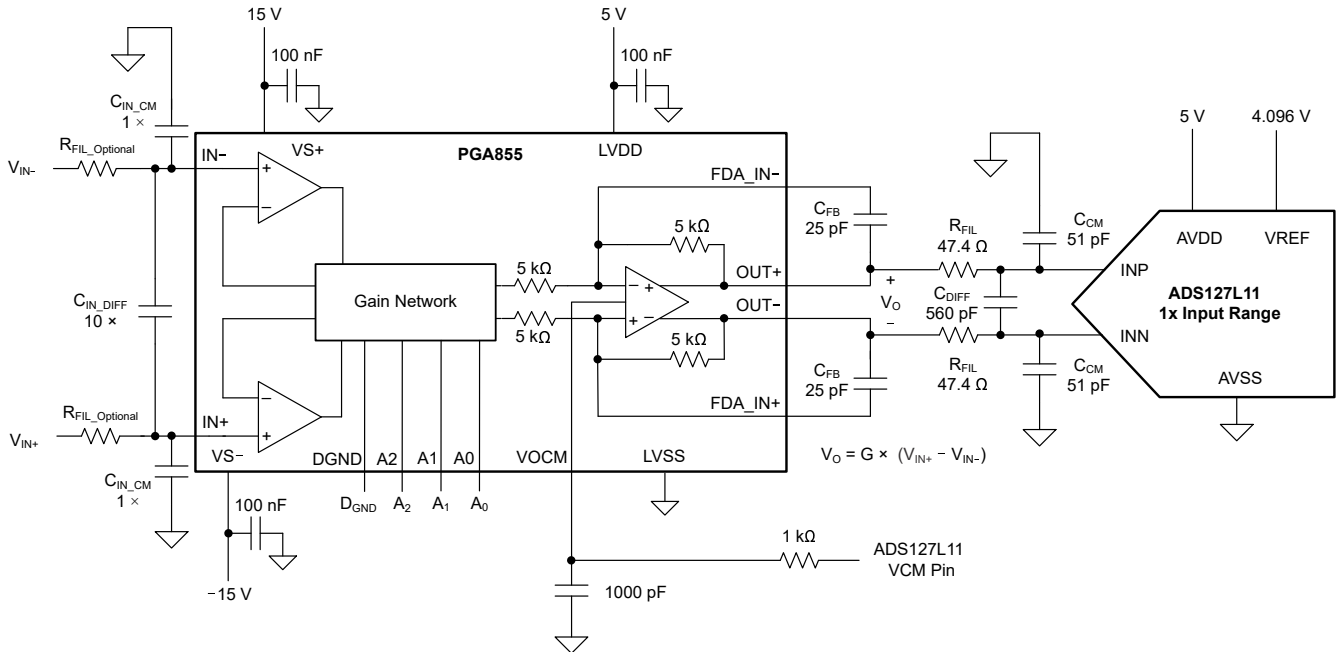


**Figure 9-6. Driving the ADS127Lx1 Delta-Sigma ADC**

#### 9.2.1.1 Design Requirements

The design requirements for the application driving the [ADS127Lx1](#) ADC are listed in the following table.

**Table 9-1. Design Parameters**

PARAMETER	VALUE
Differential-to-differential conversion	$V_{INDIFF}$ to $V_{OUTDIFF}$
Supply voltages	$V_{S\pm} = \pm 15$ V, $V_{LVDD} = 5$ V, $V_{LVSS} = \text{GND}$ , $V_{REF} = 4.096$ V
Full-scale range of ADC	$\text{FSR} = \pm 4.096$ V
Data rate of ADC	$f_{\text{DATA}} = 187.5$ kSPS
ADC filter configuration	(1) High-speed mode, Sinc4 filter, $\text{OSR} = 64$
	(2) High-speed mode, Wideband filter, $\text{OSR} = 64$
PGA gain	See <a href="#">Table 9-2</a> and <a href="#">Table 9-3</a>
Signal frequency	Tested at $f_{\text{IN}} = 1$ kHz
RC kickback filter <sup>(1)</sup>	$R_{\text{FIL}} = 47.4$ Ω, $C_{\text{DIFF}} = 560$ pF, $C_{\text{CM}} = 51$ pF

- (1) Consider a trade-off between THD, frequency response, and drift. The differential current drift into the ADC can interact with the filter resistors and result in higher drift errors. However, lower resistance degrades the phase margin of the PGA855. For low drift applications, keep  $R_{\text{FIL}} < 50$  Ω.

### 9.2.1.2 Detailed Design Procedure

表 9-2 和 表 9-3 show the typical signal-to-noise (SNR) and total harmonic distortion (THD) of the PGA855 driving the ADS127Lx1 delta-sigma ADC using a sinc4 or wideband filter. 図 9-7 和 図 9-8 show the respective FFT plots. For the SNR and THD measurements, a 1-kHz differential signal is applied. The signal amplitude is adjusted to produce a PGA855 output at  $-0.2$  dBFS of the ADC full-scale range. For a list of the equivalent input voltage amplitude signals for the different PGA855 gain configurations, see 表 9-2 and 表 9-3. At gain = 1 V/V, the design achieves  $-121.4$ -dB THD and 109.1-dB SNR.

**表 9-2. PGA855 and ADS127Lx1 FFT Data Summary, OSR = 64, Sinc4 Filter**

PGA GAIN (V/V)	INPUT AMPLITUDE (V <sub>PP</sub> )	SNR (dB)	THD (dB)	ENOB (Bits)
0.125	40.0	106.0	-119.6	17.5
0.25	32.022	109.0	-119.3	17.8
0.5	16.012	109.8	-121.2	17.9
1	8.006	109.6	-121.4	17.9
2	4.002	109.6	-121.4	17.9
4	2.002	107.4	-121.4	17.5
8	1.0	104.0	-121.4	17.0
16	0.5	99.1	-117.0	16.2

**表 9-3. PGA855 and ADS127Lx1 FFT Data Summary, OSR = 64, Wideband Filter**

PGA GAIN (V/V)	INPUT AMPLITUDE (V <sub>PP</sub> )	SNR (dB)	THD (dB)	ENOB (Bits)
0.125	40.0	106.0	-119.6	17.3
0.25	32.022	107.5	-119.0	17.5
0.5	16.012	107.7	-121.2	17.6
1	8.006	107.6	-121.4	17.6
2	4.002	107.0	-121.4	17.5
4	2.002	105.4	-121.4	17.2
8	1.0	101.7	-121.4	16.6
16	0.5	96.7	-117.0	15.8

The R-C-R differential low-pass filter at the input of the instrumentation amplifier helps reduce EMI/RFI high-frequency extrinsic noise. This filter can be customized per the bandwidth and application requirements. This design example (see [Figure 9-6](#)) suggests a filter with the capacitor ratio of  $C_{IN\_DIFF} = 10 \times C_{IN\_CM}$ . Using the 10-to-1 ratio for differential capacitor  $C_{IN\_DIFF}$  versus common-mode capacitors  $C_{IN\_CM}$  offers good differential and common-mode noise rejection, and this arrangement tends to be less sensitive to the tolerance variation and mismatch of the filter capacitors.

The feedback capacitor,  $C_{FB}$ , is in parallel with the PGA855 output-stage 5-k $\Omega$  feedback resistors to implement additional noise filtering. The internal resistors have  $\pm 15\%$  absolute resistance variation, and this variation must be taken in to account when implementing noise filtering. In this example,  $C_{FB}$  is set to 25 pF, providing a typical  $f_{-3dB}$  corner frequency of 1 MHz. The estimated minimum  $f_{-3dB}$  corner frequency for this circuit is approximately 938 kHz when accounting for the feedback-resistor variation.

The filter at the ADS127Lx1 inputs works as a charge reservoir to filter the sampled input of the ADC. The charge reservoir reduces the instantaneous charge demand of the amplifier, maintaining low distortion and low gain error that otherwise can degrade because of incomplete amplifier settling. The ADC input filter values are  $R_{FIL} = 47.4\ \Omega$ ,  $C_{DIFF} = 560\ \text{pF}$ , and  $C_{CM} = 51\ \text{pF}$ . The ADC input precharge buffers significantly reduce the sample-phase input charge that raises the ADC input impedance to decrease gain error.

High-grade COG (NPO) are used everywhere in the signal path ( $C_{IN\_DIFF}$ ,  $C_{IN\_CM}$ ,  $C_{FB}$ ,  $C_{DIFF}$ ,  $C_{CM}$ ) for low distortion. Among ceramic surface-mount capacitors, COG (NPO) ceramic capacitors provide the best capacitance accuracy. The type of dielectric used in COG (NPO) ceramic capacitors provides the most stable electrical properties over voltage, frequency, and temperature changes.

### 9.2.1.3 Application Curves

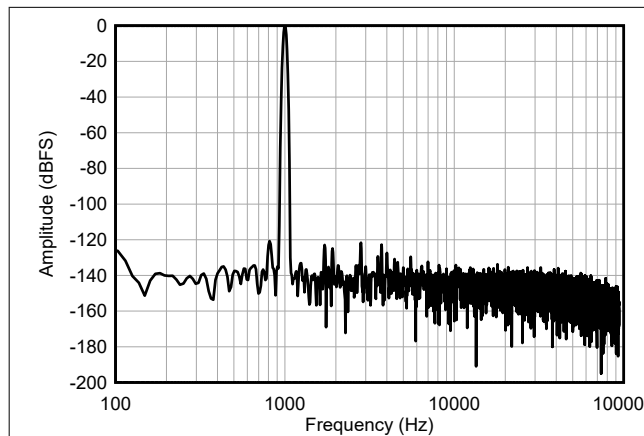


**Figure 9-7. Performance FFT Plots With ADS127L11, OSR = 64, Sinc4 Filter**

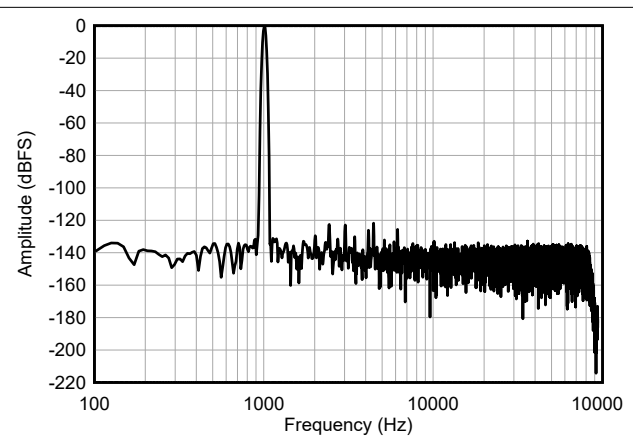


**Figure 9-8. Performance FFT Plots With ADS127L11, OSR = 64, Wideband Filter**

## 9.2.2 ADS8900B 20-Bit SAR ADC Driver Circuit

The application circuit in [Figure 9-9](#) shows the schematic for the 20-bit, precision, 1-MSPS, successive approximation register (SAR), analog-to-digital converter (ADC). This circuit is used to measure the driving capability of the PGA855 with the [ADS8900B](#) ADC. The circuit accepts single-ended or differential input signals.

The PGA855 operates with independent input and output power supplies. In this example,  $\pm 15\text{-V}$  power supplies are used for the input section, and a  $5.3\text{-V}$  power supply for the output section.

To reduce extrinsic voltage supply noise, the ADC portion of the circuit uses the [TPS7A4700](#), a low-noise,  $4\text{-}\mu\text{VRMS}$  LDO voltage regulator, to generate a unipolar  $5.3\text{-V}$  ADC supply rail and the PGA855 output stage supply is powered by the same  $5.3\text{-V}$  ADC supply. The  $5.3\text{-V}$  output supply operation prevents overloading the ADC inputs during PGA overdrive conditions. The [REF5050](#) is selected as a voltage reference; this is a low-noise, low-drift, precision  $5\text{-V}$  reference connected to the ADS8900B REFIN pin.

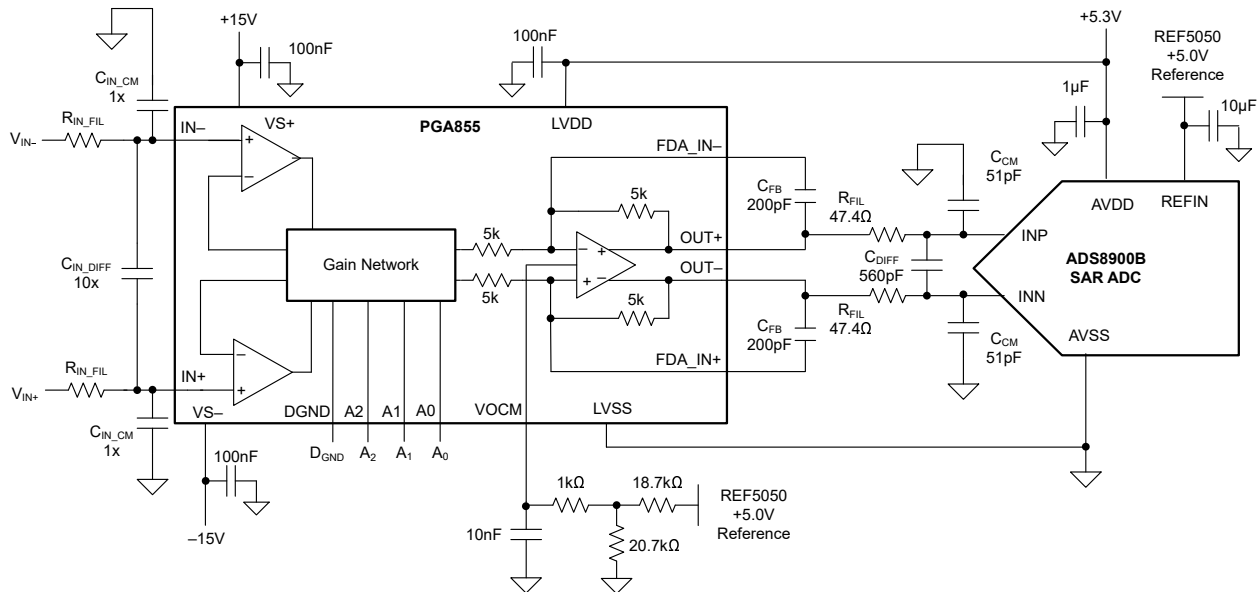


**Figure 9-9. Driving the SAR ADC ADS8900B**

### 9.2.2.1 Design Requirements

The design requirements for the application driving the ADS8900B ADC are listed in the following table.

**Table 9-4. Design Parameters**

PARAMETER	VALUE
Supply voltages	$V_{S\pm} = \pm 15\text{ V}$ , $V_{LVDD} = 5.3\text{ V}$ , $V_{LVSS} = \text{GND}$ , $V_{REF} = 5\text{ V}$
Full-scale range of ADC	$\text{FSR} = \pm 5\text{ V}$
Sampling rate of ADC	$f_{\text{SAMPLE}} = 1\text{ MSPS}$
PGA gain	See <a href="#">Table 9-5</a>
Input signal amplitude	See <a href="#">Table 9-5</a>
Signal frequency	Tested at $f_{\text{IN}} = 1\text{ kHz}$
RC kickback filter	$R_{\text{FIL}} = 47.4\ \Omega$ , $C_{\text{DIFF}} = 560\text{ pF}$ , $C_{\text{CM}} = 51\text{ pF}$

### 9.2.2.2 Detailed Design Procedure

The ADS8900B requires an input common-mode voltage within the range of  $V_{REF} / 2 \pm 100\text{ mV}$ . The PGA855 VOXM pin is set to a nominal voltage of approximately  $2.58\text{ V}$ . The VOXM voltage is purposely set to a voltage slightly greater than  $V_{REF} / 2$  to maximize the output voltage swing range of the PGA855, while allowing margin for the VOXM offset voltage error and drift variation. The VOXM voltage is generated by feeding the REF5050

reference through an 18.7 k $\Omega$ - to 0 k $\Omega$  voltage divider implemented with 0.1% tolerance resistors. An additional RC filter with R = 1 k $\Omega$ , C = 10 nF is used in close proximity to the VO<sub>CM</sub> pin as shown on [Figure 9-9](#).

The R-C-R differential low-pass filter at the input of the PGA helps reduce EMI/RFI high frequency extrinsic noise. This filter can be customized per the bandwidth and application requirements.

Two first-order filters are implemented with the PGA855 circuit. The first filter is provided by C<sub>FB</sub> in parallel with the PGA 5-k $\Omega$  feedback resistors. The PGA resistors are  $\pm 15\%$  absolute tolerance, such as, consider the effect of the tolerance on the filter cutoff frequency, the filter frequency changes to 126 kHz. At this tolerance, the filter maintains  $-0.1$  dB flatness to 24 kHz.

There is flexibility of modifying the C<sub>FB</sub> capacitor value to adjust bandwidth, with the trade-off on the broadband noise of the circuit.

The second filter placed directly at the ADS8900B inputs works as a charge reservoir to filter the sampled input of the ADC. The charge reservoir reduces the instantaneous charge demand of the amplifier, maintaining low distortion that otherwise can degrade because of incomplete amplifier settling. The RC filter combination (R<sub>FIL</sub>, C<sub>DIFF</sub>) is optimized for the SAR ADC sample and hold settling. This combination reduces nonlinear charge kickback of the SAR ADC and is optimized for best THD performance. This combination allows for the best trade-off between harmonic distortion while maintaining stability of the PGA output stage.

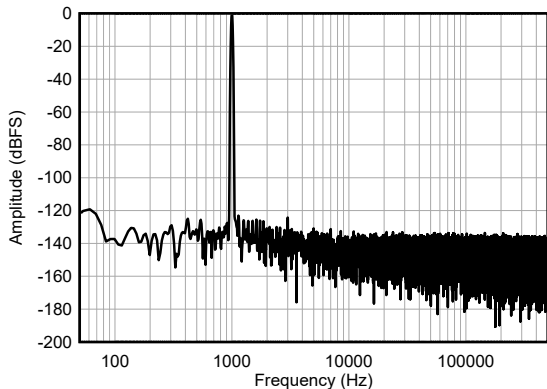
High-grade C0G (NPO) are used everywhere in the signal path (C<sub>IN\_DIFF</sub>, C<sub>IN\_CM</sub>, C<sub>FB</sub>, C<sub>DIFF</sub>, C<sub>CM</sub>) for the low distortion properties.

The results are shown in [Table 9-5](#), which includes the typical signal-to-noise ratio (SNR) and total harmonic distortion (THD) of the PGA855 driving the ADS8900B SAR ADC. For the SNR and THD measurements, a 1-kHz differential signal is applied. The signal amplitude is adjusted to produce a PGA855 output at  $-0.5$  dBFS of the ADC full-scale range. [Table 9-5](#) shows the equivalent input voltage amplitude signal for different PGA855 gain configurations. At gain = 1 V/V, the design achieves a  $-121.4$ -dB THD and 101.2-dB SNR.

**表 9-5. PGA855 and ADS8900B FFT Data Summary: f<sub>SAMPLE</sub> = 1 MSPS, f<sub>IN</sub> = 1 kHz**

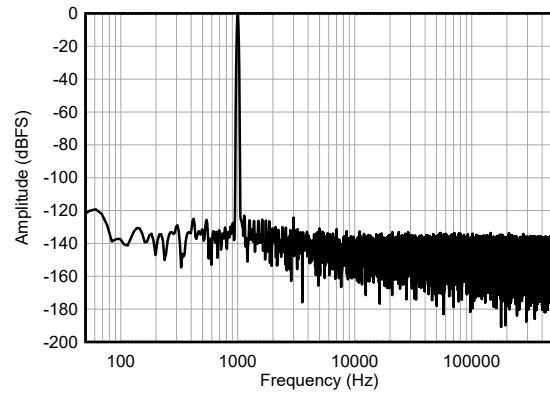
PGA GAIN (V/V)	INPUT AMPLITUDE (V <sub>PP</sub> )	ADC SIGNAL POWER (dBFS)	SNR (dB)	THD (dB)	ENOB (Bits)
0.125	40.10	-6.0	95.9	-118.2	15.6
0.25	36.48	-0.8	101.0	-118.6	16.5
0.5	18.24	-0.8	101.2	-121.0	16.5
1	9.12	-0.8	101.2	-121.7	16.5
2	4.56	-0.8	100.5	-121.6	16.4
4	2.28	-0.8	99.5	-121.3	16.2
8	1.14	-0.8	97.4	-119.4	15.9
16	0.58	-0.8	93.6	-117.3	15.2

### 9.2.2.3 Application Curves



Gain = 1 V/V,  $f_{\text{SAMPLE}} = 1 \text{ MSPS}$ ,  $f_{\text{IN}} = 1 \text{ kHz}$

 **9-10. Performance FFT Plot With ADS8900B**



Gain = 4 V/V,  $f_{\text{SAMPLE}} = 1 \text{ MSPS}$ ,  $f_{\text{IN}} = 1 \text{ kHz}$

 **9-11. Performance FFT Plot With ADS8900B**



## 9.3 Power Supply Recommendations

The nominal performance of the PGA855 is specified with input-stage supply and output-stage supply voltages of  $\pm 15$  V, and  $V_{ICM}$  and  $V_{OCM}$  at mid-supply. Within the specified limits, custom input and output common-mode voltages can be used without compromising performance; see also [セクション 7.3](#).

### 注意

To prevent damage to internal circuitry, the output-stage power supplies are clamped to stay within the input-stage supply voltage levels; see [セクション 8.2](#).

## 9.4 Layout

### 9.4.1 Layout Guidelines

Attention to good layout practices is always recommended. For best operational performance of the device, use good PCB layout practices, including:

- To avoid converting common-mode signals into differential signals and thermal electromotive forces (EMFs), make sure that both input paths are symmetrical and well-matched for source impedance and capacitance.
- Noise can propagate into analog circuitry through the power pins of the device and of the circuit as a whole. Bypass capacitors reduce the coupled noise by providing low-impedance power sources local to the analog circuitry.
  - Connect low-ESR, 0.1- $\mu$ F ceramic bypass capacitors between each supply pin and ground, placed as close as possible to the device. A single bypass capacitor from  $V_{S+}$  and  $V_{LVDD}$  to ground is applicable for single-supply applications.
- To reduce parasitic coupling, run the input traces as far away as possible from the supply or output traces. If these traces cannot be kept separate, crossing the sensitive trace perpendicular is much better than in parallel with the noisy trace.
- Leakage on the FDA\_IN+ and FDA\_IN– pins can cause in a dc offset error in the output voltages. Additionally, excessive parasitic capacitance at these pins can result in decreased phase margin and affect the stability of the output stage. If these pins are not used to implement deliberate capacitive feedback, follow best practices to minimize leakage and parasitic capacitance.
- Follow best practices to minimize leakage and parasitic capacitance, which includes implementing *keep-out* areas in any ground planes that lie immediately below the input pins.
- Minimize the number of thermal junctions. If possible, route the signal path using a single layer without vias.
- Keep sufficient distance from major thermal energy sources (circuits with high power dissipation). If not possible, place the device so that the effects of the thermal energy source on the high and low sides of the differential signal path are evenly matched.
- Keep the traces as short as possible.

### 9.4.2 Layout Example

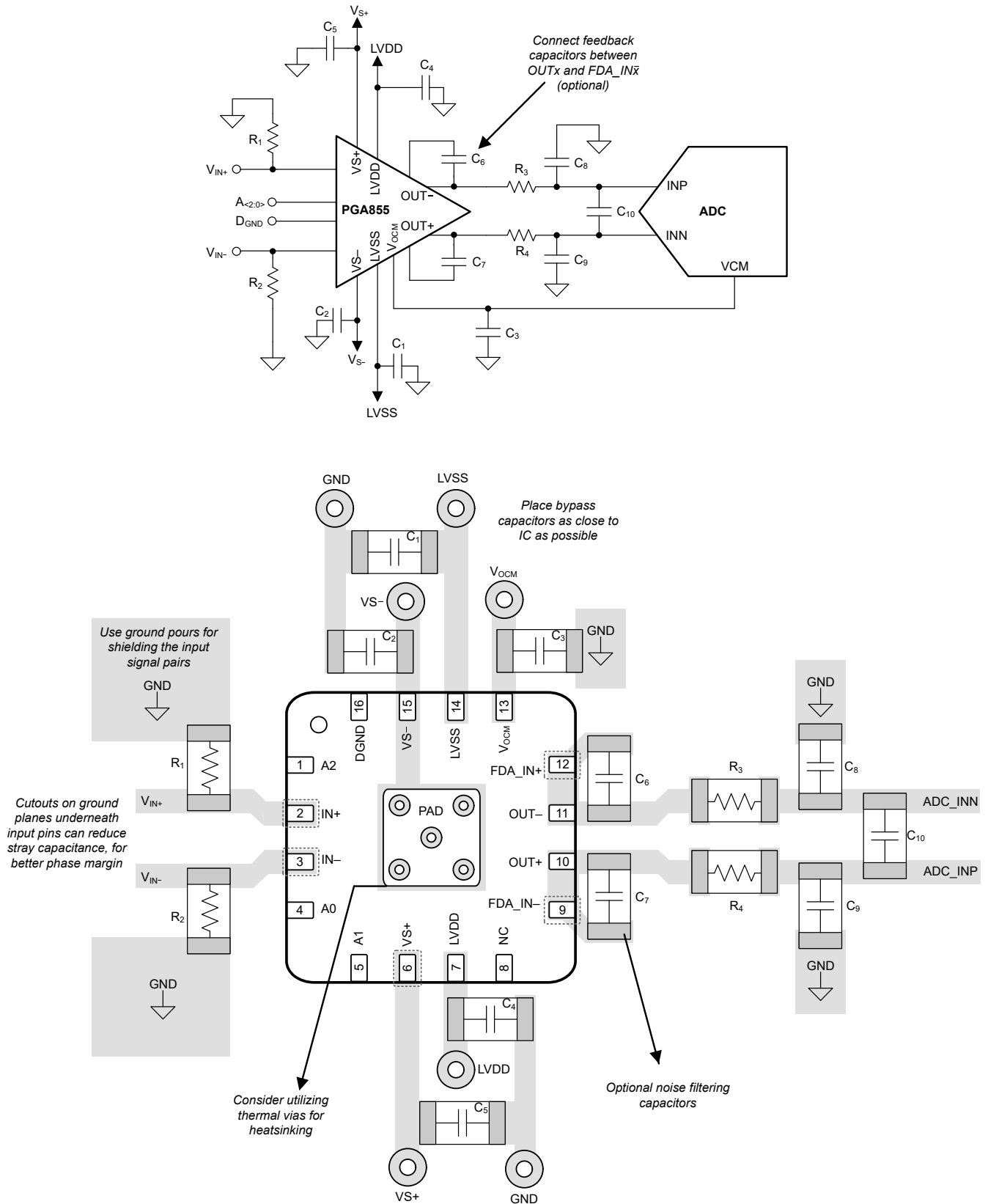


図 9-12. Example Schematic and Associated PCB Layout

## 10 Device and Documentation Support

### 10.1 Device Support

#### 10.1.1 Development Support

##### 10.1.1.1 PSpice® for TI

PSpice® for TI is a design and simulation environment that helps evaluate performance of analog circuits. Create subsystem designs and prototype solutions before committing to layout and fabrication, reducing development cost and time to market.

### 10.2 Documentation Support

#### 10.2.1 Related Documentation

For related documentation see the following:

- Texas Instruments, [Comprehensive Error Calculation for Instrumentation Amplifiers application note](#)
- Texas Instruments, [Importance of Input Bias Current Return Paths in Instrumentation Amplifier Applications application note](#)

### 10.3 ドキュメントの更新通知を受け取る方法

ドキュメントの更新についての通知を受け取るには、[ti.com](#) のデバイス製品フォルダを開いてください。「更新の通知を受け取る」をクリックして登録すると、変更されたすべての製品情報に関するダイジェストを毎週受け取れます。変更の詳細については、修正されたドキュメントに含まれている改訂履歴をご覧ください。

### 10.4 サポート・リソース

TI E2E™ サポート・フォーラムは、エンジニアが検証済みの回答と設計に関するヒントをエキスパートから迅速かつ直接得ることができる場所です。既存の回答を検索したり、独自の質問をしたりすることで、設計に必要な支援を迅速に得ることができます。

リンクされているコンテンツは、該当する貢献者により、現状のまま提供されるものです。これらは TI の仕様を構成するものではなく、必ずしも TI の見解を反映したものではありません。TI の [使用条件](#) を参照してください。

### 10.5 Trademarks

TI E2E™ is a trademark of Texas Instruments.

PSpice® is a registered trademark of Cadence Design Systems, Inc.

すべての商標は、それぞれの所有者に帰属します。

### 10.6 静電気放電に関する注意事項



この IC は、ESD によって破損する可能性があります。テキサス・インスツルメンツは、IC を取り扱う際には常に適切な注意を払うことを推奨します。正しい取り扱いおよび設置手順に従わない場合、デバイスを破損するおそれがあります。

ESD による破損は、わずかな性能低下からデバイスの完全な故障まで多岐にわたります。精密な IC の場合、パラメータがわずかに変化するだけで公表されている仕様から外れる可能性があるため、破損が発生しやすくなっています。

### 10.7 用語集

[テキサス・インスツルメンツ用語集](#) この用語集には、用語や略語の一覧および定義が記載されています。

## 11 Mechanical, Packaging, and Orderable Information

The following pages include mechanical, packaging, and orderable information. This information is the most current data available for the designated devices. This data is subject to change without notice and revision of this document. For browser-based versions of this data sheet, refer to the left-hand navigation.

**PACKAGING INFORMATION**

Orderable Device	Status (1)	Package Type	Package Drawing	Pins	Package Qty	Eco Plan (2)	Lead finish/ Ball material (6)	MSL Peak Temp (3)	Op Temp (°C)	Device Marking (4/5)	Samples
PGA855RGTR	ACTIVE	VQFN	RGT	16	3000	RoHS & Green	NIPDAU	Level-1-260C-UNLIM	-40 to 125	PGA855	Samples

(1) The marketing status values are defined as follows:

**ACTIVE:** Product device recommended for new designs.

**LIFEBUY:** TI has announced that the device will be discontinued, and a lifetime-buy period is in effect.

**NRND:** Not recommended for new designs. Device is in production to support existing customers, but TI does not recommend using this part in a new design.

**PREVIEW:** Device has been announced but is not in production. Samples may or may not be available.

**OBSOLETE:** TI has discontinued the production of the device.

(2) **RoHS:** TI defines "RoHS" to mean semiconductor products that are compliant with the current EU RoHS requirements for all 10 RoHS substances, including the requirement that RoHS substance do not exceed 0.1% by weight in homogeneous materials. Where designed to be soldered at high temperatures, "RoHS" products are suitable for use in specified lead-free processes. TI may reference these types of products as "Pb-Free".

**RoHS Exempt:** TI defines "RoHS Exempt" to mean products that contain lead but are compliant with EU RoHS pursuant to a specific EU RoHS exemption.

**Green:** TI defines "Green" to mean the content of Chlorine (Cl) and Bromine (Br) based flame retardants meet JS709B low halogen requirements of <=1000ppm threshold. Antimony trioxide based flame retardants must also meet the <=1000ppm threshold requirement.

(3) MSL, Peak Temp. - The Moisture Sensitivity Level rating according to the JEDEC industry standard classifications, and peak solder temperature.

(4) There may be additional marking, which relates to the logo, the lot trace code information, or the environmental category on the device.

(5) Multiple Device Markings will be inside parentheses. Only one Device Marking contained in parentheses and separated by a "~" will appear on a device. If a line is indented then it is a continuation of the previous line and the two combined represent the entire Device Marking for that device.

(6) Lead finish/Ball material - Orderable Devices may have multiple material finish options. Finish options are separated by a vertical ruled line. Lead finish/Ball material values may wrap to two lines if the finish value exceeds the maximum column width.

**Important Information and Disclaimer:** The information provided on this page represents TI's knowledge and belief as of the date that it is provided. TI bases its knowledge and belief on information provided by third parties, and makes no representation or warranty as to the accuracy of such information. Efforts are underway to better integrate information from third parties. TI has taken and continues to take reasonable steps to provide representative and accurate information but may not have conducted destructive testing or chemical analysis on incoming materials and chemicals. TI and TI suppliers consider certain information to be proprietary, and thus CAS numbers and other limited information may not be available for release.

In no event shall TI's liability arising out of such information exceed the total purchase price of the TI part(s) at issue in this document sold by TI to Customer on an annual basis.

**TAPE AND REEL INFORMATION**

**QUADRANT ASSIGNMENTS FOR PIN 1 ORIENTATION IN TAPE**


\*All dimensions are nominal

Device	Package Type	Package Drawing	Pins	SPQ	Reel Diameter (mm)	Reel Width W1 (mm)	A0 (mm)	B0 (mm)	K0 (mm)	P1 (mm)	W (mm)	Pin1 Quadrant
PGA855RGTR	VQFN	RGT	16	3000	330.0	12.4	3.3	3.3	1.1	8.0	12.0	Q2

**TAPE AND REEL BOX DIMENSIONS**


\*All dimensions are nominal

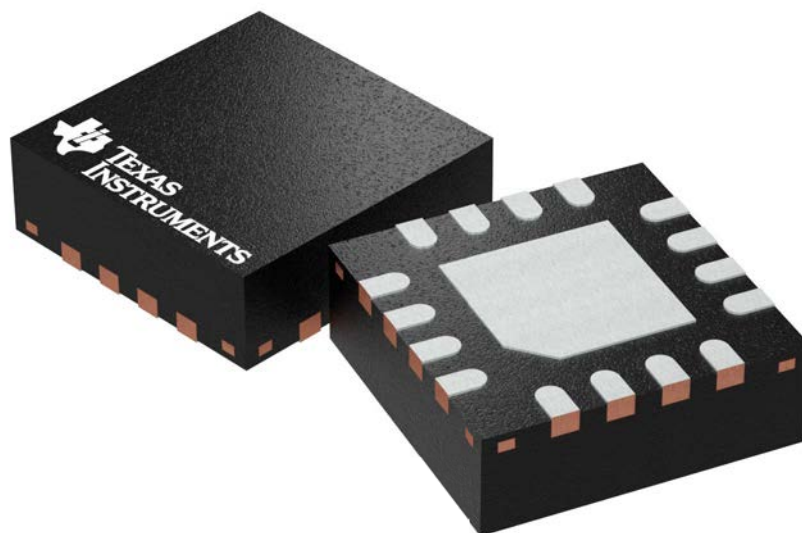
Device	Package Type	Package Drawing	Pins	SPQ	Length (mm)	Width (mm)	Height (mm)
PGA855RGTR	VQFN	RGT	16	3000	367.0	367.0	35.0

**RGT 16**

**GENERIC PACKAGE VIEW**

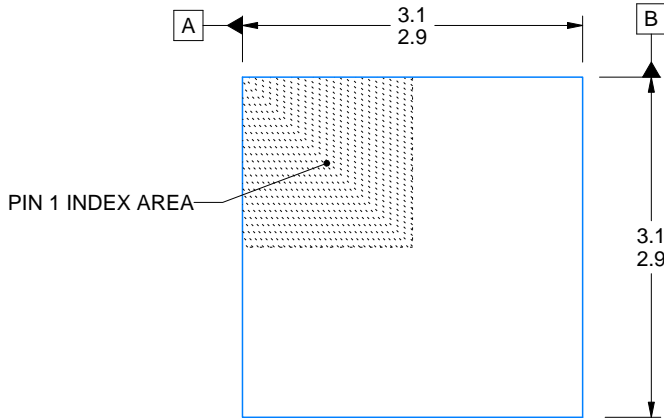
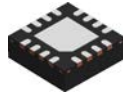
**VQFN - 1 mm max height**

PLASTIC QUAD FLATPACK - NO LEAD

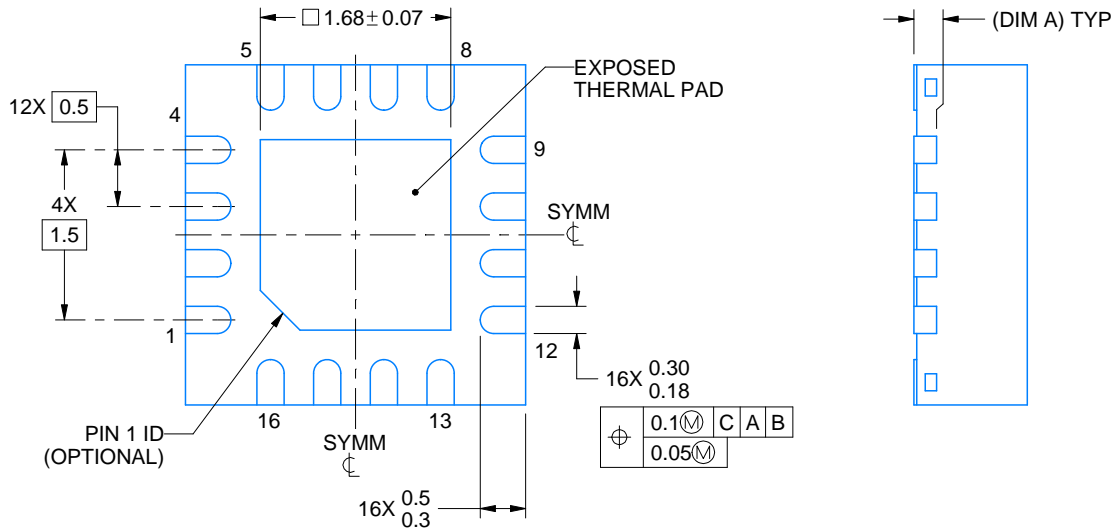
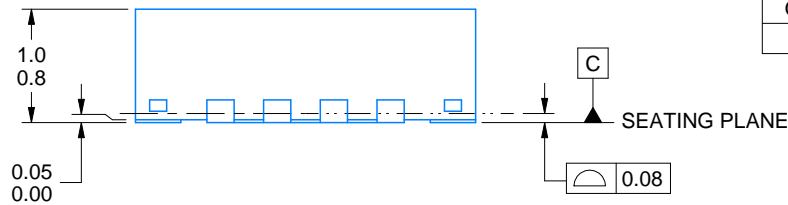


Images above are just a representation of the package family, actual package may vary.  
Refer to the product data sheet for package details.

4203495/1



SIDE WALL METAL THICKNESS DIM A	
OPTION 1	OPTION 2
0.1	0.2



4222419/D 04/2022

NOTES:

1. All linear dimensions are in millimeters. Any dimensions in parenthesis are for reference only. Dimensioning and tolerancing per ASME Y14.5M.
2. This drawing is subject to change without notice.
3. The package thermal pad must be soldered to the printed circuit board for thermal and mechanical performance.

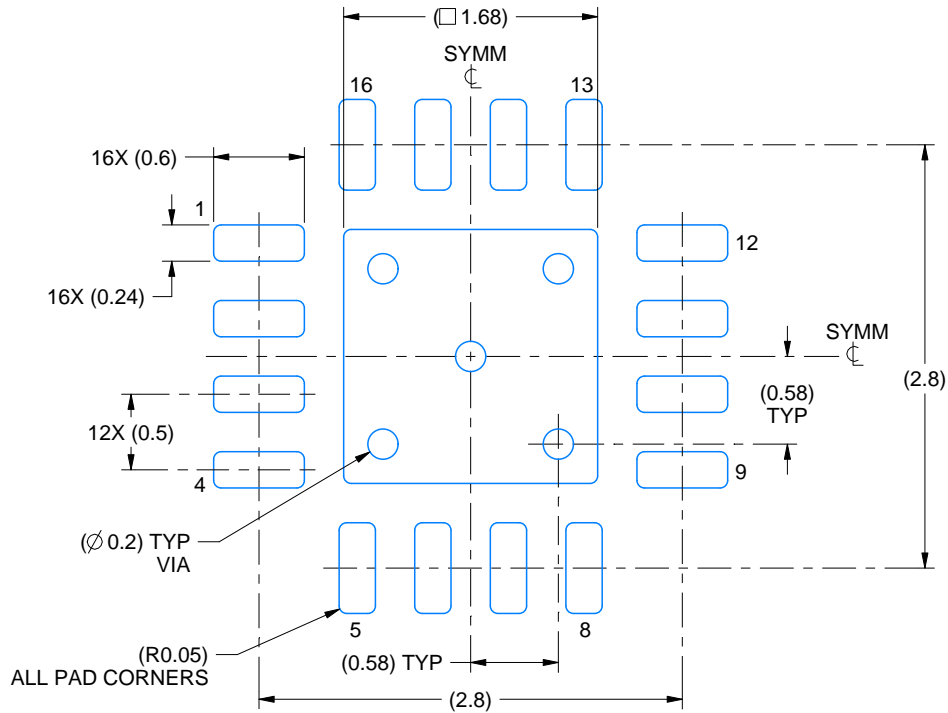


# EXAMPLE BOARD LAYOUT

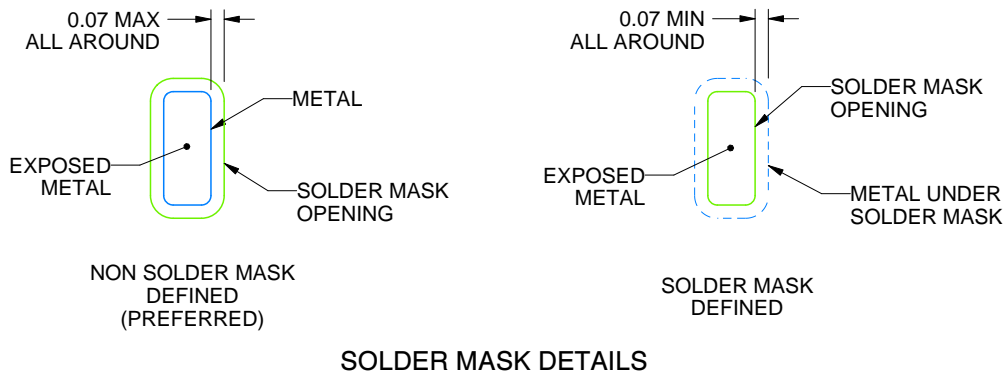
RGT0016C

VQFN - 1 mm max height

PLASTIC QUAD FLATPACK - NO LEAD



LAND PATTERN EXAMPLE  
EXPOSED METAL SHOWN  
SCALE:20X



SOLDER MASK DETAILS

4222419/D 04/2022

NOTES: (continued)

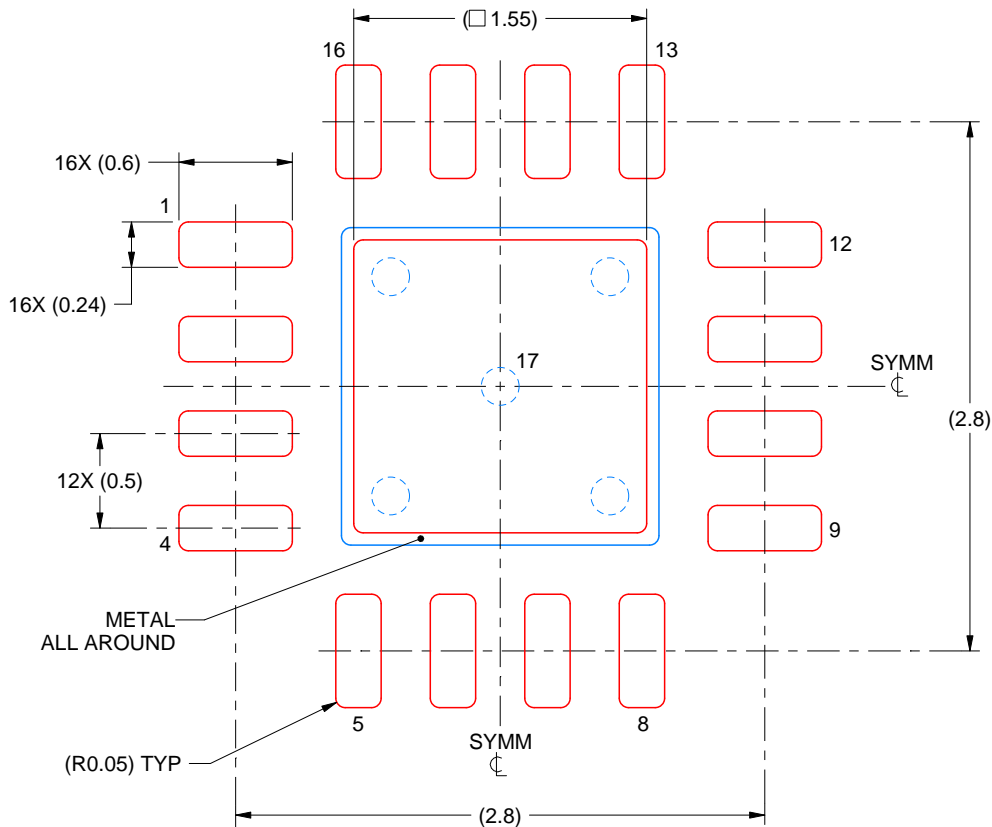
4. This package is designed to be soldered to a thermal pad on the board. For more information, see Texas Instruments literature number SLUA271 ([www.ti.com/lit/slua271](http://www.ti.com/lit/slua271)).
5. Vias are optional depending on application, refer to device data sheet. If any vias are implemented, refer to their locations shown on this view. It is recommended that vias under paste be filled, plugged or tented.

# EXAMPLE STENCIL DESIGN

RGT0016C

VQFN - 1 mm max height

PLASTIC QUAD FLATPACK - NO LEAD



**SOLDER PASTE EXAMPLE**  
BASED ON 0.125 mm THICK STENCIL

EXPOSED PAD 17:  
85% PRINTED SOLDER COVERAGE BY AREA UNDER PACKAGE  
SCALE:25X

4222419/D 04/2022

NOTES: (continued)

6. Laser cutting apertures with trapezoidal walls and rounded corners may offer better paste release. IPC-7525 may have alternate design recommendations.

## 重要なお知らせと免責事項

TI は、技術データと信頼性データ(データシートを含みます)、設計リソース(リファレンス・デザインを含みます)、アプリケーションや設計に関する各種アドバイス、Web ツール、安全性情報、その他のリソースを、欠陥が存在する可能性のある「現状のまま」提供しており、商品性および特定目的に対する適合性の黙示保証、第三者の知的財産権の非侵害保証を含むいかなる保証も、明示的または黙示的にかかわらず拒否します。

これらのリソースは、TI 製品を使用する設計の経験を積んだ開発者への提供を意図したものです。(1) お客様のアプリケーションに適した TI 製品の選定、(2) お客様のアプリケーションの設計、検証、試験、(3) お客様のアプリケーションに該当する各種規格や、その他のあらゆる安全性、セキュリティ、規制、または他の要件への確実な適合に関する責任を、お客様のみが単独で負うものとします。

上記の各種リソースは、予告なく変更される可能性があります。これらのリソースは、リソースで説明されている TI 製品を使用するアプリケーションの開発の目的でのみ、TI はその使用をお客様に許諾します。これらのリソースに関して、他の目的で複製することや掲載することは禁止されています。TI や第三者の知的財産権のライセンスが付与されている訳ではありません。お客様は、これらのリソースを自身で使用した結果発生するあらゆる申し立て、損害、費用、損失、責任について、TI およびその代理人を完全に補償するものとし、TI は一切の責任を拒否します。

TI の製品は、[TI の販売条件](#)、または [ti.com](#) やかかる TI 製品の関連資料などのいずれかを通じて提供する適用可能な条項の下で提供されています。TI がこれらのリソースを提供することは、適用される TI の保証または他の保証の放棄の拡大や変更を意味するものではありません。

お客様がいかなる追加条項または代替条項を提案した場合でも、TI はそれらに異議を唱え、拒否します。

郵送先住所 : Texas Instruments, Post Office Box 655303, Dallas, Texas 75265  
Copyright © 2024, Texas Instruments Incorporated